Cytometry
PART A
Journal of the International Society for Advancement of Cytometry

Multiplexed Imaging of Intracellular Protein Networks

Hernán E. Grecco,[1] Sarah Imtiaz,[2] Eli Zamir[2]*

[1]Department of Physics, FCEN, University of Buenos Aires and IFIBA, CONICET, Buenos Aires, Argentina

[2]Department of Systemic Cell Biology, Max Planck Institute of Molecular Physiology, Dortmund, Germany

Received 3 December 2015; Revised 21 April 2016; Accepted 26 April 2016

*Correspondence to: Eli Zamir, Department of Systemic Cell Biology, Max Planck Institute of Molecular Physiology, Dortmund, Germany. E-mail: eli.zamir@mpi-dortmund.mpg.de

Published online 00 Month 2016 in Wiley Online Library (wileyonlinelibrary.com)

DOI: 10.1002/cyto.a.22876

• **Abstract**

Cellular functions emerge from the collective action of a large number of different proteins. Understanding how these protein networks operate requires monitoring their components in intact cells. Due to intercellular and intracellular molecular variability, it is important to monitor simultaneously multiple components at high spatiotemporal resolution. However, inherent trade-offs narrow the boundaries of achievable multiplexed imaging. Pushing these boundaries is essential for a better understanding of cellular processes. Here the motivations, challenges and approaches for multiplexed imaging of intracellular protein networks are discussed. © 2016 International Society for Advancement of Cytometry

• **Key terms**

multicolor imaging; high-throughput microscopy; multispectral imaging; spectral unmixing; immunofluorescence; fluorescent proteins; cyclic immunofluorescence; live cell imaging; cell-to-cell variability; spatial organization

Introduction

Understanding cellular processes requires identifying the involved biochemical components, finding out how these components affect each other and inferring how such causality network gives rise to functionality (1,2). The intracellular components conducting and regulating cellular functions include proteins, as well as lipids (e.g., phosphatidylinositol 3,4-bisphosphate), ions (e.g., Ca^{2+}), small inorganic molecules (e.g., H_2O_2), small organic molecules (e.g., retinoic acid), and RNAs (e.g., microRNAs) (3–8). These components can affect each other via direct interactions causing changes in their levels and states. In the case of a protein, the state attributes include its level, post-translational modifications (PTMs), conformation and interactions. Ultimately, such attributes have to be monitored for all the key components of a protein network in order to resolve how it works. However, it is insufficient to measure these parameters one by one in different cells, since considerable molecular variability exists between cells. One kind of cell-to-cell variability is between different types of cells within the same organism (e.g., fibroblasts, epithelial cells, different types of leukocytes, and cancer cells) that differentiated to have distinct gene expression profiles (9,10). Also included in this kind of variability are cells at different stages along a developmental lineage (11). Another kind of variability is between cells of the same type having different protein levels and states in response to different environmental conditions or different stages of a cellular process such as proliferation or adhesion. Such variability is commonly referred as extrinsic noise. Finally, cell-to-cell variability is also generated by intrinsic stochastic fluctuations (hence termed intrinsic noise), mainly in gene expression levels (12,13). Importantly, cell-to-cell variability at the molecular level can alter qualitatively the properties of a given protein network and consequently the cellular phonotype (13–17). Therefore, monitoring one component per cell would not be sufficient for uncovering the different states of the protein net-

ISAC
International Society for Advancement of Cytometry

work nor what underlies the distinct cellular behaviors. In order to overcome and utilize this diversity, it is essential to measure multiple components within the same cell (18–21).

A powerful method to quantify multiple components per cell is flow cytometry (FCM), in which cells in a fluid stream are measured one by one as they flow through a beam of light (22–24). Using just the scattering of light, multiple properties can be measured such as their size and granularity. More importantly, with the aid of fluorescently labeled specific antibodies, the levels of multiple proteins can be quantified in single cells (25). FCM can also quantify per cell the levels of multiple PTMs, such as phosphorylation, using specific antibodies (26,27). Thus, FCM can be used to quantify changes in the state of multiple proteins in response to stimuli or differences in the state of proteins between cell populations (28–30). Importantly, in FCM the fluorescence signal is integrated over the whole cell. Therefore FCM excels at measuring with a good signal to noise ratio a large number of single cells in a very short time. Nevertheless, the spectral width of available fluorophores poses a practical limit to the number of components that can be simultaneously measured by FCM. Tandem dyes, consisting of a covalently bound Förster resonance energy transfer (FRET) donor fluorophore (e.g., allophycocyanin) and acceptor fluorophores, enable to achieve a variety of Stokes shifts between the excitation and emission spectra. Thus, tandem dyes facilitate the detection of multiple components using one excitation laser wavelength (31–33). Phycoerythrin (PE) and allophycocyanin (APC) are being commonly used as donor fluorophores in these tandem dyes due to their brightness (32,34,35). The usage of spatially separated excitation beams further facilitates the multiplexity in FCM. Due to its multiplexity and throughput, FCM pioneered quantification of multiple components in single cells. Still, due to the spectral overlap between fluorophores, the FCM multiplexity is currently limited to around 18 different components—proteins or phosphorylation states (36). Mass cytometry overcomes the spectral limitation of FCM by using time-of-flight mass spectrometry, instead of fluorescence measurements, to quantify the abundance of multiple components in single cells (37–48). In this technique, antibodies which are linked to rare earth metal isotopes (metal tags) are used to label the proteins of interest and the cells are nebulized one by one to mass spectrometric analysis. State-of-the-art mass cytometers can distinguish up to 100 different metal tags, however, their multiplexed implementation is practically limited by the number of tags that are available in high purity, currently around 40 (37,44,45).

Along the signal-to-noise advantage in FCM and mass cytometry, achieved by whole-cell signal integration, comes inevitably a limitation—the lack of spatial information. Only limited spatial information could be derived by FCM and only in case that the labeling is compartment-specific, particularly monitoring the surface levels of proteins using cell impermeable labels. Therefore, FCM and mass cytometry are mostly valuable for studying protein networks in cases where changes in protein localization do not take place or at least are not essential for the operation of the network. However, in many cases the spatial organization of proteins and its changes in response to signals are critical for the function of intracellular protein networks (49). First, in steady-state the spatial distributions of protein levels and activities is inhomogeneous within the cell and dynamically maintained far from equilibrium to form intracellular localization patterns needed for the cell functions. Furthermore, signals rapidly change the steady-state spatial patterns of many proteins and activities within the cell (50). For example, the activity of proteins can vary between the cytoplasm and the nucleus as well as between the front and rear edges of a migrating cell. Similarly, the molecular composition of intracellular structures and organelles can vary within an individual cell (51–55). Such spatial organization of protein networks within a cell can change rapidly in response to cues, as a key mode of signaling, information processing, conceiving spatial information and generating spatial patterns (49,56,57). Therefore, for revealing how protein networks operate their components should be monitored at high spatial and temporal resolutions within the cells. Importantly, measuring one component per object (i.e., a structure or an organelle) cannot reveal the compositional diversity between them. Therefore, multiplexed imaging is required in order to monitor the levels of multiple components at subcellular resolutions.

A method termed imaging mass spectrometry enables imaging high number of proteins and their phosphorylation states in tissues. In this approach, spatial resolution is achieved by localized sampling of a tissue specimen with an ionizing laser beam (58–63). The resulting ions are transferred to the mass spectrometer, for the identification of the molecular content in the sampled spot. Subsequently, a next spot at a defined distance in this specimen gets equivalently sampled and analyzed, and so on repeatedly till the whole area of interest is raster-scanned. In addition to the unprecedented power of imaging mass spectrometry in quantifying a large number of components, it has a critical advantage that it does not require specific labeling of the components. On the other hand, a current drawback of imaging mass spectrometry is its low spatial resolution (typically > 10 μm), in comparison to light-based imaging. Therefore, although mass spectrometry can identify hundreds of components in a pool of intracellular structures upon fractionation or enrichment, it currently cannot achieve this for individual structures, such as cell–matrix adhesion sites (64,65). In addition, imaging mass spectrometry is destructive for the sample and hence inherently cannot be used to follow dynamic processes in the same cell.

Fluorescence microscopy enables the imaging of multiple components (referred hereafter as multiplexed imaging) in live cells at high spatial and temporal resolutions. As such, it is an essential tool for studying complex intracellular processes. Multiplexed imaging enables not only overcoming intercellular and intracellular heterogeneities in molecular content, but also resolving these heterogeneities spatiotemporally and utilizing them as a source of information. Furthermore, multiplexed imaging facilitates sensitive coupled comparisons between the dynamics and spatial distributions of two or more components. A coupled comparison between

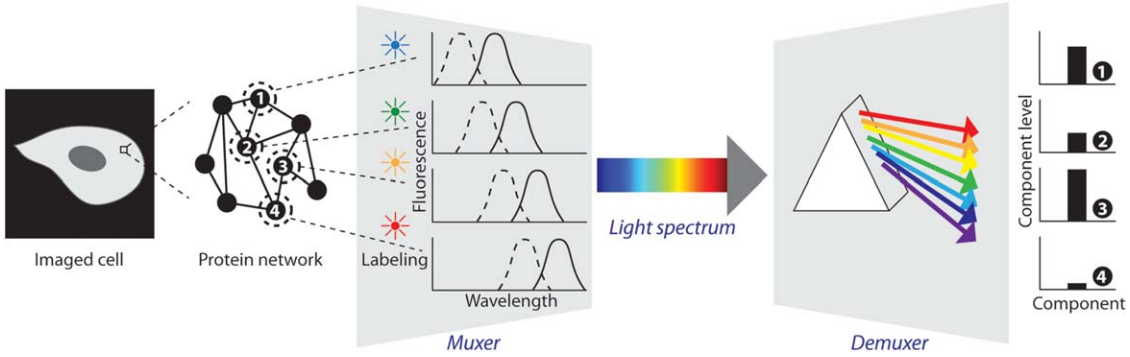

Figure 1. Imaging and multiplexing. The concept of multiplexing refers to the transmission of multiple messages via a single communication channel. In this terminology, the section that convolves the multiple messages onto one channel is called muxer, while demuxer is the section that after transmission retrieves the original messages. Accordingly, multiplexed imaging refers to the imaging of multiple components in the same cell via a single channel—the light spectrum. The messages are the levels of different components in each resolvable voxel in the cell. These messages are encoded by labeling the components with fluorophores, which generates for each pixel an integrative, mixed, emission and excitation spectra. From these mixed spectra, the relative levels of each component in each pixel are resolved by optical (e.g., filters) or computational (e.g., linear unmixing) approaches. [Color figure can be viewed in the online issue which is available at wileyonlinelibrary.com]

components in the same object (cell, organelle, a structure, or a pixel) enables to detect temporal and spatial differences that are smaller than the abovementioned inter- and intracellular variability. In this review we discuss the fundamental challenges for multiplexed imaging and the current approaches to address them.

Fundamental Trade-Offs In Multiplexed Imaging

The term "multiplexing" was coined for telecommunication systems that transmit several messages via the same channel (66). Since this term became widely adopted also for the co-imaging of multiple components in cells, it is noteworthy explaining the analogy. The first step in multiplexing is encoding the different input messages into one message in the communication channel by a device termed muxer. Following transmission of this message, a demuxer retrieves from it the multiple original messages (Fig. 1). In multiplexed imaging, the equivalent of the muxer are the labeling tools used to label different cellular components with different fluorophores. Thus, the levels of these components in each pixel are encoded in one mixed message—the integrative excitation and emission spectra (Fig. 1). The demuxer in multiplexed imaging consists of the optical and computational instrumentations that derive the level of each labeled component from the integrative spectra. Beside the terminology aspect, conceiving co-imaging of multiple components as a multiplexing process provides a general formulation of the challenge and types of solutions. Accordingly, the fundamental challenge in multiplexed imaging is how to encode information about the levels of multiple components using a single medium, light, with specificity, sensitivity, spatio-temporal resolution, and sufficient throughput (67).

Spectrally tunable excitation and detection is the first important aspect for achieving multiplexed imaging. Light emitting diodes (LED) illumination, combined with optical filter sets to select and isolate the excitation and emission light, are broadly used to achieve multiplexed imaging. Two types of filter sets provide alternative solutions to achieve multiple imaging channels, named after their originators. "Pinkel" filter set consists of multiple single-bandpass excitation filters and a single multibandpass emission filter. Such filter sets enable high-speed multiplexed imaging, as only the excitation filters have to be changed in a filter wheel while the multiband beamsplitter and emission filter are fixed. "Sedat" filter sets consist of multiple single-bandpass excitation filters and multiple single-bandpass emission filters. These filter sets can provide the highest signal-to-noise ratio for a given combination of fluorophores, while still enabling rapid sequential acquisition of each of the color. QUAD-Sedat or QUAD-Pinkel filter sets are optimized for multiplexed imaging of blue, green, orange, and red light emitting fluorophores. Penta-Sedat or Penta-Pinkel filter set enables multiplexed imaging of blue, green, orange, red, and infrared emitting fluorophores. Beside filters with fixed optical properties, spectral filtering can be achieved also with acousto-optical tunable filter (AOTF) and acousto-optic beam splitters (AOBS) that use radiofrequency sound waves to diffract and shift light. AOTF enables to control the range of transmitted light wavelength via changing the frequency of sound waves. Similarly to AOTF, liquid crystal tunable filters (LCTF) enable to control the wavelength range of transmitted light via changing the applied electric potential. Both AOTF and LCTF provide a fast and flexible mean to spectrally control the light path, thus to design optimal acquisition setups for multiplexed imaging. In comparison, AOTF enables a faster spectral selection while LCTF provides a better photon collocation and thus a better signal-to-noise ratio.

The photophysical properties of fluorophores that are directly relevant for multiplexed imaging are their spectral attributes, as they determine the capability to obtain a specific signal from a given fluorophore in the presence of other given fluorophores in the sample. The larger is the separation between the excitation or emission spectra of the two fluorophores, the larger signal can be collected from them without bleed-through. However, as we increase the number of

components to be co-imaged, the spectral overlap between the fluorophores labeling them inevitably increases. Sequential imaging, that is, exciting and detecting each fluorophore one after the other, can be used to reduce crosstalk at the expense of a longer imaging time. But this only mildly mitigates the problem for highly spectrally overlapping fluorophores. Another way to cope with spectral overlap is to narrow-down the spectral-detection range of emitted light wavelengths collected by the detectors for each fluorophore, thus to avoid bleed-through. Similarly, a sub-optimal wavelength for the excitation of a given fluorophore might be used in order to decrease dramatically the degree of excitation of the other used fluorophores. Both of these solutions cause a reduction in the amount of emitted photons collected from each fluorophore for a given dose of excitation light, in comparison to the optimal acquisition setups if that fluorophore would had been used alone.

Additional photophysical properties of fluorophores important for multiplexed imaging are the extinction coefficient and quantum yield. The extinction coefficient (ε) is a wavelength-dependent property that determines its capability to absorb light. Measured at the peak of the extinction spectrum, its value ranges from 10^3 to 10^5 in $\mathrm{Mol}^{-1}\ \mathrm{cm}^{-1}$ for typical fluorophores used in fluorescence microscopy, but can be larger than $10^6\ \mathrm{Mol}^{-1}\ \mathrm{cm}^{-1}$ for quantum dots (68). While ε is related to the probability to absorb excitation energy, the quantum yield (QY) indicates the probability that such energy is emitted as photons. A higher QY implies that the fluorescent protein provides a higher number of emitted photons per a given excitation dose, thus may provide a sufficient signal even with sub-optimal excitation and emission setups. Importantly, a lower QY usually leads to a larger generation of reactive oxygen species, which affect signaling and cause phototoxicity (69–72). Together, the extinction coefficient and QY determine the brightness of the fluorophore. However, it is convenient to define the effective brightness for a fluorophore m in a particular imaging channel n as:

$$b_{\mathrm{m,n}} = \left(\int_0^\infty L_{\mathrm{n}}(\lambda)\, U_{\mathrm{n}}(\lambda)\, \varepsilon_{\mathrm{m}}(\lambda)\, d\lambda\right) \times QY_{\mathrm{m}} \left(\int_0^\infty F_{\mathrm{m}}(\lambda)\, V_{\mathrm{n}}(\lambda)\, D_{\mathrm{n}}(\lambda)\, d\lambda\right) \quad (1)$$

where the first and last terms are related to the probability of exciting the fluorophore and detecting its fluorescence, respectively [Eq. (1)]. In more detail, and related to the imaging channel n, $L_{\mathrm{n}}(\lambda)$ is the spectrum of the light source (e.g., lamp, laser), $D_{\mathrm{n}}(\lambda)$ is the spectral sensitivity of the detector (e.g., camera, photomultiplier tube), $U_{\mathrm{n}}(\lambda)$ and $V_{\mathrm{n}}(\lambda)$ are the transmission spectra of the filters in the emission and excitation paths, respectively (taken in a generic sense, as the spectral filtering might be achieved with other elements such as a monochromator or AOTF). Related to the fluorophore, and in addition to the previously described ε and QY, $F_{\mathrm{m}}(\lambda)$ describes the emission spectrum.

Another important parameter for multiplexed imaging is the photostability of the fluorophores. A more photostable protein would tolerate better a higher dose of excitation light before getting gradually and irreversibly bleached. Therefore, higher photostability enables to compensate for the sub-optimal collection of emitted photons in multiplexed imaging by increasing the intensity of the excitation light. Photostability is particularly important when imaging dynamic processes, as otherwise significant photobleaching might occur before the monitored process is concluded. Another more subtle, and therefore obstructing, effect of poor photostability is the differential photobleaching of distinct species, leading to inaccurate determination of the stoichiometry over time.

The signal in each pixel (i, j) for a given channel n is the product of the brightness and the concentration of fluorescent molecules:

$$S_{\mathrm{n,i,j}} = \sum_{\mathrm{m}} C_{\mathrm{m,i,j}}\, b_{\mathrm{m,n}} \quad (2)$$

Equation (2) illustrates the challenge to achieve multicolor imaging. The effective brightness is potentially not null for all combinations of fluorophores and imaging channels. In other words, for a cell transfected with green and red fluorescent proteins (e.g., GFP and RFP) and an imaging system with two channels (named Green and Red), the fluorescence of GFP will be visible in the red channel (i.e., brightness $b_{\mathrm{GFP,RED}} > 0$).

An identity between imaging channels and fluorophores is achieved only if $b_{\mathrm{m,n}}$ is diagonal (i.e., have non-null values only when m=n). In such a case, imaging of each component does not contain any bleed-through from the other channels and therefore the acquired image can be directly interpreted as the intensity levels of this component. In cases where $b_{\mathrm{m,n}}$ is not diagonal, computational methods to extract the "fluorophore signal" from the "imaging channel signal" have to be used. Such computational approaches are called spectral unmixing (73–78) and involve inverting the problem to obtain $C_{\mathrm{m,i,j}}$ from $b_{\mathrm{m,n}}$ and $S_{\mathrm{n,i,j}}$. In other words, finding which combinations of fluorophores sum up to the measured spectra in a given pixel. The possibility to perform this calculation is directly related to the ability to invert the matrix $b_{\mathrm{m,n}}$—that is, a unique concentration vector C will be obtained if the equations represented in matrix b are linearly independent. The most widely used implementation of spectral unmixing involves determining first the spectral fingerprint (or signature) of all fluorescent species using a set of pure samples, that is, samples labeled with a single fluorophore. By measuring them with the same imaging channels used in the experiment, the matrix $b_{\mathrm{m,n}}$ can be experimentally determined. The same can be achieved without the need of pure sample, if pixels containing signal from only one fluorophore are present and identifiable in the image. Finally, the abundance of the different fluorophores in each pixel $C_{\mathrm{m,i,j}}$ can be then obtained by using any of the established algebraic methods such as inverting $b_{\mathrm{m,n}}$. This calculation becomes more sensitive to noise and prone to errors as a function of the number of fluorophores, their spectral overlap, their spatial overlap and the differences in their local relative abundances. In such cases, inverting $b_{\mathrm{m,n}}$ might yield meaningless negative concentration values. Therefore, bounded minimization methods, such as non-negative least square, are in many

occasions more appropriate. These methods are also convenient when the number of channels is larger than the number of fluorophores, since such a system is over-determined and might be inconsistent due to the presence of noise. In certain cases, the spectral fingerprint of one or more species cannot be easily determined independently in pure samples. This is quite common in remote sensing applications but can also occur in fluorescence microscopy with autofluorescence. In such cases, methods that infer the spectral fingerprint from the data, such as principle component analysis and supervised classification analysis, could be used (79,80). Notably, analyzing simultaneously, in a single model, spectral mixing, optical blurring and detection noise has been demonstrated to provide better sensitivity and accuracy in comparison to sequential considerations of these aspects (81).

An important practical consideration in choosing between the spectral handling approaches for multiplexed imaging is whether the goal is to identify spatially separated structures (such as distinct chromosomes in metaphase or distinct organelles) or alternatively to quantitatively compare the molecular content of structures (such as adhesion sites). In the former case, each object (e.g., a chromosome) retains its spectral signature, which could be resulting from a single fluorophore or from several fluorophores with a relatively fixed stoichiometry. Since these objects are spatially separated, their signatures do not mix during detection and therefore many objects with distinct signatures could be discriminated and identified with high accuracy and sensitivity. Thus, for example, spectral karyotyping (SKY) and multiplexed fluorescence in-situ hybridization (M-FISH) can identify all chromosomes and many chromosomal aberrations using combinatorial labeling scheme combined with either Fourier spectroscopy or filter-based spectra measurements, respectively (82–87). In general, multispectral imaging approaches are more powerful in differentiating between spectral signatures, as they measure the whole spectra rather than sampling a few number of regions of it. However, if the multiplexed imaging goal is to quantitatively compare and monitor the molecular composition of structures, then there are no discrete spectral signatures but rather mixed spectra that must be accurately unmixed to retrieve the level of each fluorophore in each pixel. As abovementioned, this task becomes less and less feasible the more fluorophores are being used or the more incomparable is there levels in a given structure. Therefore, in practice, multispectral imaging is more suited for imaging a large number of components that are mostly non-overlapping within the cell, or different types of structures having each a rather fixed stoichiometry of the labeled components. On the other hand, for imaging multiple components that are co-localized within the same intracellular structure, it is often required to use fluorophores that can be spectrally separated pre-acquisition.

As can be concluded, multiplexed imaging has trade-offs with the signal to noise ratio—either because of reducing the number of collected photons to avoid bleed-through or because of error levels in calculating the contribution of each fluorophore to the mixed spectrum in each pixel. Therefore, it is challenging to combine multiplexity with other aspects of imaging which by themselves also reduce the signal to noise ratio: spatial resolution, temporal resolution, and throughput (Fig. 2a). A higher spatial resolution implies a lower copy number of the label components in each resolvable area unit and therefore a lower signal. A higher temporal resolution implies a lower integration time, therefore a lower number of photons and signal-to-noise ratio. This integration time is confined not only by the required sampling rate but also by the need to avoid bleaching, which is particularly important in time-lapse live cell imaging. High-throughput requires fast acquisition and therefore motivates minimization of the integration time. Different techniques set different compromise points along the trade-offs between multiplexity, spatial resolution, and temporal resolution (Fig. 2b). Some of these techniques, particularly imaging-based, enable a relative freedom in setting the trade-off points according to the particular needs of the given experiment.

Multiplexed Imaging Of Proteins In Fixed Cells

Live cell imaging is limited by the need to label the intracellular components without harming or affecting the cells. Imaging fixed cells is not subjected to such limitation, allowing for post-fixation and permeabilization labeling of the components of interest. This is particularly helpful for multiplexed imaging since it enables the use of antibodies conjugated with organic fluorophores for the labeling of specific proteins within the cell. The brightness and photostability of organic dyes are in general higher than those of fluorescent proteins, thus enabling to obtain images with a higher signal-to-noise ratio. Another important advantage of immunofluorescence, in comparison to fluorescent proteins, is the ability to monitor directly PTMs, for example, by using phospho-specific antibodies. Since the activity of many proteins depends on their PTMs, immunofluorescence thus enables imaging the active states of multiple components in the same cell.

In addition to organic fluorophores, during the last 15 years quantum dots have become an important class of fluorescent labels for imaging cells (88–95). Quantum dots are semiconductor nanocrystals with several unique and useful photophysical properties: (i) they are by far brighter and more photostable than organic dyes and fluorescent proteins, (ii) their emission spectra is relatively narrow and tunable, being more red-shifted as the size of the quantum dot is bigger, (iii) their excitation spectra is common, regardless of their emission spectra, enabling exciting them all simultaneously with a 405 nm laser line. Surface functionalization of quantum dots enables to attach them to peptides and proteins, such as antibodies (96). These properties make quantum dots valuable for multiplexed imaging, particularly in fixed and permeablized cells (88–90,94,96–102). Since the size of antibody-quantum dots conjugate is considerably bigger than that of antibody-organic dye conjugate (94), the accessibility of the former to the target epitops within the cell should be carefully evaluated for each particular application. The large size of quantum dots (6–60 nm), in comparison to organic dyes (~0.5 nm) also

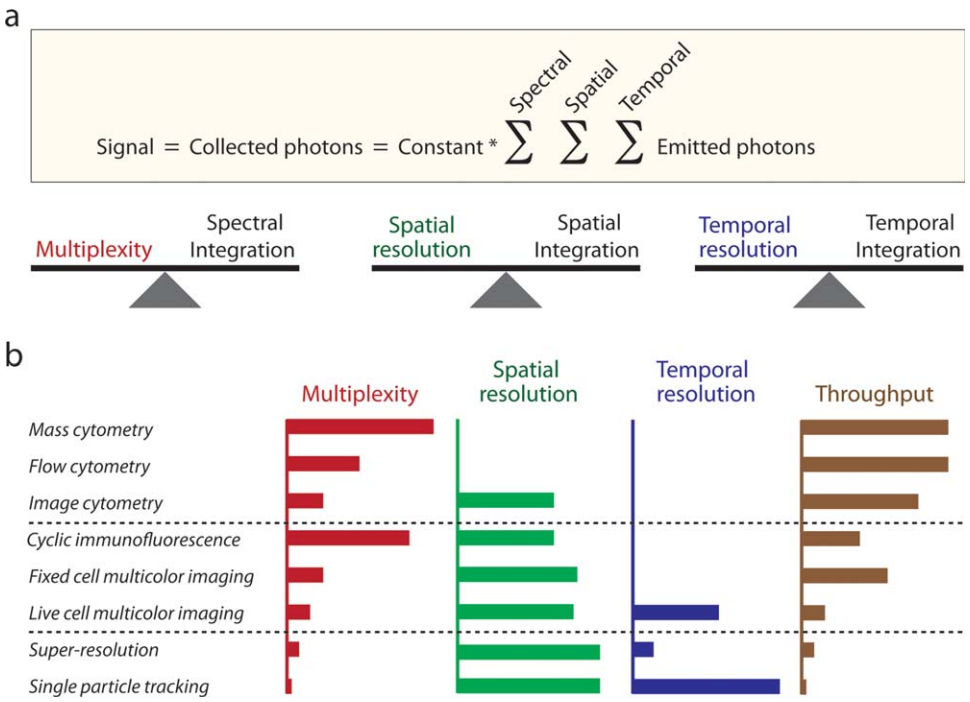

Figure 2. Imaging trade-offs. (**a**) The signal in imaging is the number of photons collected per each resolvable space-time unit, thus is proportional to the range of wavelengths within which emitted photons are being collected (spectral integration), the size of the resolvable area (or volume) in the sample from which emitted photons are collected (spatial integration) and the time duration during which emitted photons are collected (temporal integration). Higher multiplexing reduces spectral integration, as it imposes narrowing it down to avoid bleed-through or using noise-sensitive spectral unmixing calculations. Higher spatial and temporal resolutions reduce the spatial and temporal integrations, respectively. Thus, it is challenging to achieve sufficient signal levels in multiplexed imaging at high spatial and temporal resolutions. (**b**) A qualitative comparison between different cytometry and imaging approaches according to their typical multiplexity, spatial resolution, temporal resolution and throughput. [Color figure can be viewed in the online issue which is available at wileyonlinelibrary.com]

challenges their applicability in live cells, as it requires their insertion into the cell by microinjection or other techniques.

Although the photophysical properties of organic fluorophores and quantum dots are in general better than that of fluorescent proteins for multiplexed imaging, spectral overlap is still a limiting factor for increasing the number of co-imaged components in fixed cells. In direct immunofluorescence, in which the primary antibodies are directly labeled, the spectral overlap is the main fundamental limitation for multiplexed imaging, although in practice the limitation is often the availability of primary antibodies against the proteins of interest that are conjugated with spectrally separable fluorophores. Multiplexed imaging using indirect immunofluorescence is limited by the need to avoid cross-reactivity of the secondary antibodies with the used primary antibodies. This is usually addressed by using primary antibodies from different host species, such as mouse, goat, and rabbit, and secondary antibodies that are specific to the antibodies of a given species. Therefore, the number of components that can be co-immunolabeled is in practice confined by the availability of primary antibodies from different host species and of secondary antibodies that are conjugated with spectrally separable fluorophores. This number can be further increased by combining immunofluorescence with other labeling approaches, such as fluorescently tagged small molecules (e.g., phalloidin for the labeling of actin filaments) and genetic tagging with fluorescent proteins (53,103). In addition, multiple different primary antibodies from the same host species can be used together by pre-complexing each of them separately with fluorescently labeled Fab fragments that bind their Fc domain (53). Thus for example, by combining the abovementioned labeling approaches, multiplexed imaging of five components of cell–matrix adhesion sites in fixed fibroblasts was achieved (Fig. 3) (53).

An important approach for multiplexed imaging of fixed cells that overcomes the limitations caused by spectral overlap is cyclic immunofluorescence (also called toponome imaging). This approach is based on serial cycles of immunolabeling, imaging, and photobleaching or chemical inactivation of the fluorophore or protease-mediated antibody stripping (104–112). Thus, the same fluorophore, or set of fluorophores, can be used repeatedly to label multiple components within the same cell. So far this approach was applied mainly using fluorescently labeled primary antibodies, thus overcoming the problem of cross-reactivity between secondary and primary antibodies. Also, the imaged components were mostly cell-surface ones (113–117), which makes the labeling and washout of the unbound antibodies more feasible. In this way, cyclic immunofluorescence can enable to image around a hundred of different components in the same cells and tissue (118). Noteworthy, cyclic immunofluorescence was applied also on intracellular components, yet in a relatively low multiplexity (119,120). In order to broaden the applicability of

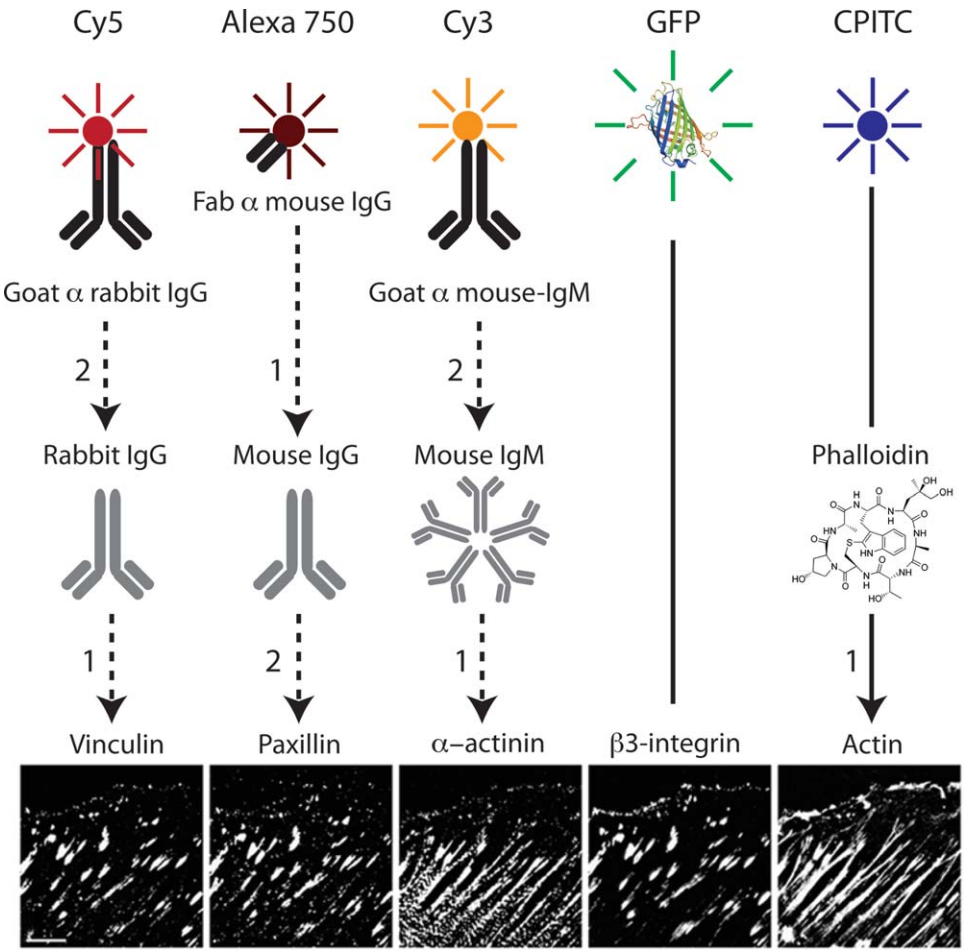

Figure 3. Five-color imaging of components of cell-matrix adhesion sites in fixed cells. Labeling of five different components in fixed REF52 cells was achieved by combining different labeling approaches and fluorophores: (i) actin filaments were labeled via CPITC-conjugated phalloidin, (ii) β3-integrin-GFP integrin was stably expressed in these cells, hence enabling the imaging of this component, (iii) α-actinin was labeled using mouse IgM anti-α-actinin followed by an isotype-specific Cy3-conjugated goat anti mouse-IgM, antibody (iv) paxillin was labeled with mouse IgG anti-paxillin pre-complexed with Alexa-750-conjugated Fab fragments, (iv) vinculin was labeled by rabbit IgG anti-vinculin followed by Cy5-conjugated goat-anti-rabbit IgG. The arrows are numbered according to the order by which the reagents were joined along the labeling procedure of each component. Note that the five components are localized largely in the same structures, posing a bigger challenge for multiplexed imaging, in comparisons with cases in which the components are spatially separated. Scale bar, 10 μm. Reproduced with modifications from Zamir et al. 2008 (53). [Color figure can be viewed in the online issue which is available at wileyonlinelibrary.com]

cyclic immunofluorescence imaging for the study of large intracellular protein networks, it would be important to optimize labeling protocols and instrumentation for cycling the immunolabeling of intracellular proteins. Cyclic immunofluorescence offers a generic solution for multiplexed imaging of fixed cells. Yet, it requires a large set of labeled primary antibodies, long staining and washout cycles and verifying that the accessibility of antibodies to their epitopes is retained.

Live Cell Multiplexed Imaging

Early imaging studies of proteins in live cells were based on microinjecting these proteins, fluorescently labeled, into cells (121–126). These studies monitored mostly only one component within a cell, plausibly due to the technical difficulties of purifying, labeling and microinjecting functional proteins. The discovery and first implementations of the green fluorescent protein as a tool in cell biology (127–131) revolutionized the feasibility to monitor the spatiotemporal dynamics of proteins within live cells. However, as long as only one fluorescent protein was available, multiplexed imaging required a combination with other techniques of labeling, such as immunofluorescence (55). During the last 15 years, extensive research has been conducted to isolate fluorescent proteins from various organisms and mutate them to generate proteins with a variety of photophysical properties (132–138). Two-color live cell imaging with two spectrally separated fluorophores can be performed without a significant loss of signal, in comparison of using each of the fluorophores separately in different cells (135). However, due to the relative wide excitation and emission spectra of fluorescent proteins within the total light spectrum range, a three-color live cell imaging

requires already narrowing down the range of collected emission wavelengths to avoid bleed-through. The extent of spectral overlap increases dramatically with the addition of any further fluorophore to the labeling scheme, making it practically unfeasible to image quantitatively more than four components with sufficient sensitivity if they are all co-localized in an overlapping manner in the same intracellular structures. Of note, five component live cell imaging was achievable, for components that are localized in different cellular compartments and labeled with organic dyes (139).

An important complementary method for labeling proteins in live cells is fusing them genetically with a tag that binds specifically a cell-permeable synthetic dye (140–146). The advantages of such protein chemical labeling are the superior photophysical properties of the synthetic dyes in comparison to most fluorescent proteins, and their smaller size. The firstly developed system for such labeling consists of tetracysteine tags and fluorescein arsenical hairpin (FlAsH) binder (144). Several years later, resorufin arsenical hairpin (ReAsH), a red-emitting analog of the green-emitting FlAsH, was developed (145). Since both FlAsH and ReAsH bind to tetracysteine tags, they cannot be straightforwardly combined with each other for multiplexed imaging. Noteworthy, a sequential labeling approach, utilizing the differential affinities of two different tetracysteine tags to FlAsH and ReAsH, enabled specific dual color labeling of parathyroid hormone and β-arrestin2 (147). More generically, having the two analogs, FlAsH and ReAsH, facilitates multiplexity by providing flexibility in using one of them together with a fluorescent protein. A consecutively developed labeling system consists of the SNAP-tag and CLIP-tag that bind chemical probes with O6-benzylguanine and O2-benzylcytosine derivatives, respectively (148). Similarly, Halo-tag binds synthetic dyes having a chloroalkane linker (149–152). Furthermore, cell-permeable fluorescent probes that bind His-tag were recently developed (153). These labeling systems are orthogonal (i.e., do not crosstalk with each other) and therefore can be combined together for multiplexed imaging in live cells (154–156). Moreover, these labeling approaches facilitated super-resolution and multiplexed super-resolution imaging in live cells (154–158). In principle, combining all these aforementioned tools could allow the co-labeling of 5–6 components in live cells with synthetic dyes. However, for translating this capability to 5–6 multiplexed imaging, a broader repertoire of tag-binding dyes with distinct spectra is needed. In parallel, development of additional orthogonal tags and chemical labeling schemes would be valuable for advancing sensitive multiplexed imaging of protein networks in live cells.

Another generic method to label proteins in live cells is Fab-based live endogenous modification labeling (FabLEM) (159,160). This method is based on microinjecting fluorescently labeled specific Fab antibody fragments. Since Fab fragments, unlike the complete antibody, are monovalent they are not causing dimerization of their target cellular proteins. Yet, a considerable drawback of FabLEM is the need to insert the Fab fragments into the cell by microinjection or other techniques, such as glass beads loading (161). To overcome this, genetically encoded single-chain variable fragment of the antibody can be genetically fused with a fluorescent protein and expressed in cells (162). Important aspect that should be carefully controlled here is the possible impact of the Fab on the interactions and activities of the labeled protein, particularly since the Fab binds the protein itself and not a fused tag. Further generalization of this approach can be achieved by genetically fusing the protein of interest with SunTag and co-express it together with GFP-conjugated single chain variable antibody fragment, scFv, that binds this tag (163). Furthermore, tagging a protein with tandem repeats of SunTag provides high photon count per molecule, which is particularly valuable for single-molecule miscroscopy methods (163). Since it is possible to generate several orthogonal tag-scFv pair combinations, future developments of such tools can facilitate sensitive live cell multiplexed imaging. Yet, the effects of multiple scFv bound to tandem tags on the dynamics and localization of the target protein should be assessed carefully for each particular implementation.

Multiplexed Fluorescence-Fluctuation Measurements In Live Cells

An important class of live cell fluorescence microscopy approaches derives the information from the fluctuations of the fluorescence intensity, rather than from the level of the intensity. A major subclass of these methods includes fluorescence correlation spectroscopy (FCS) and its derivatives. In FCS, the diffusion speed and concentration of labeled species are derived by correlation analysis of their fluorescence fluctuation in a given confocal volume within the cell (164). Moreover, exemplifying the value of multiplexing at the protein–complex level, in fluorescence cross-correlation spectroscopy (FCCS), two different proteins are monitored simultaneously, enabling to infer their physical association based on co-diffusion (165–168). Recent advances in detection and spectral separation enable triple-color FCCS and thereby the monitoring of ternary protein complexes (169–172). Another subclass of fluorescence-fluctuation methods is based on analyzing the relative amplitudes of the fluctuations to derive the copy number of a protein in a complex. These number-and-brightness approaches have also been extended to two and three colors to infer the stoichiometry of protein complexes (173–175).

The basic, original, mode of data acquisition in fluorescence-fluctuation based techniques is point measurements (i.e., measuring in one spot, confocal volume) of fluorescence fluctuations at a high sampling rate (typically tens of millions times per second) within a living cell. The fast sampling of fluorescence intensity is important for capturing the intensity fluctuations as the labeled particles move into and out from the observed confocal volume. The temporal resolution of these methods is confined by the minimal integration time, along which fluorescence fluctuations are collected, that is needed to obtain a sufficient signal-to-noise ratio. Expansions of fluorescence-fluctuation based techniques achieve spatial dimension, generally by compromising on the sampling rate (hence on capturing fast diffusions), or on the temporal resolution (hence on capturing rapid changes in diffusion speed, concentrations and interactions) or on the signal-to-noise ratio (hence on capturing weak interactions and small changes in

concentrations and mobility). Such spatially resolved fluctuation methods include line scan FCS, image correlation spectroscopy (ICS), imaging FCS, raster image correlation spectroscopy (RICS) and their derivatives (176–178). Dual color implementations of these methods provide spatiotemporal information about protein complexes mobility and stoichiometry (177–181).

High multiplexing of fluorescent fluctuation methods would be valuable for the detection of high-order protein complexes—that is, complexes containing three or more proteins. A large variety of such complexes is expected to be formed in the cytosol considering the abundance of multivalent interactions within protein networks (165,182). Indeed, ternary protein complexes have been identified in few cases using biochemical and proteomic approaches (183,184). Discovering and studying high-order protein complexes in intact cells is essential for understanding signaling and structures assembly processes (184–186). However, currently the monitoring of soluble high-order protein complexes in intact live cells is challenging already for ternary complexes, being rather unfeasible for complexes with more than three components. The main cause for this difficulty is that in all fluorescence fluctuation-based methods an important parameter for a good signal is the brightness per molecule, rather than the total brightness of a structure. Therefore, narrowing the spectral integration, for a better spectral separation, reduces the signal in a way that cannot be compensated by an increase in the concentration of the labeled proteins. A practical way to address this is to use as bright fluorophores as possible and if needed, to label each protein of interest with several copies of the fluorophore, for example by tandem repeats of a fluorescent protein (165,187). From that sense, quantum dots are valuable for fluorescence fluctuation-based methods (166) and for facilitating their multiplexed implementations.

Multiplexed Super-Resolution Imaging

In order to understand how interactions between proteins give rise to the properties of an intracellular system it is important to connect their nanoscale and meso-scale spatiotemporal organizations. This line of research has become more accessible in the last two decades by the revolution of super-resolution microscopy (188–192). Yet, for revealing how the nanoscale spatiotemporal organizations of proteins relate to each other multiplexed super-resolution is required. In comparison to diffraction-limited microscopy, multiplexed imaging at a super-resolution faces additional challenges, including a higher sensitivity to chromatic aberrations due to the nanometer scale resolution and the difficulty to find compatible imaging buffers for the different fluorophores. One method to overcome these challenges is by performing cycles of labeling, STORM (stochastic optical reconstruction microscopy) imaging and fluorophore destruction (193,194). Similarly, in exchange-PAINT (point accumulation for imaging in nanoscale topography), diffusing fluorescent molecules that interact transiently with their target epitopes are being applied on the specimens for stochastic super-resolution imaging methods and then exchanged with other ones (195). Using exchange-PAINT, multiplexed super-resolution imaging of four proteins in different compartments within a fixed HeLa cell was demonstrated—β-tubulin in the microtubules, COX IV in the mitochondria, TGN46 in the Golgi, and PMP70 in peroxisomes (195). Both methods enable multiplexed super-resolution imaging of multiple targets using only one fluorophore, thereby avoiding chromatic aberrations and imaging-buffer incompatibilities. Multicolor STORM was facilitated by a combinatorial pairing of photo-switchable reporter fluorophores and shorter wavelength fluorophores that facilitates photo-activation of the reporter. Thus, the same reporter (Cy5) can be activated by spectrally distinct activators (Cy2, Cy3, and Alexa 405) or alternatively spectrally distinct reporters (Cy5, Cy5.5, and Cy7) can be activated by the same activator (Cy3), hence facilitating multiplexed STORM (196). In a more recent study, spectrally resolved STORM (SR-STORM) combined wide-field spectral measurements with photo-switching to achieve 4-color 3-dimensional multiplexed super-resolution imaging (197). Stimulated emission depletion (STED) utilizing AOTF or fixed filters for spectral separation enabled super-resolution imaging of two fluorophores in three dimensions (198,199). Multi-lifetime multi-color STED microscopy separates fluorophore signals based on both their spectra and fluorescence lifetime, thus enabling super-resolution multiplexed imaging of three proteins with a single STED beam (200).

The variety of super-resolution microscopy approaches can be also applied for multiplexed imaging in live cells (201,202). The additive challenge here is collecting fast enough separable signals from two or more fluorophores. An important advantage of single-molecule techniques facilitating multiplexed imaging is that all photons emitted during an acquisition frame can be attributed to one fluorophore, thereby providing its pure spectra and its identity. In this way, in contrast to diffraction-limited imaging, it is possible to discriminate between several emission spectra using only two detection channels (67,203–205). Thus, two-color STORM of mitochondria and the ER was performed in live cells using MitoTracker Red and ER-Tracker Red, having 16 nm separated emission spectra, using two-channel spectra sampling and a single laser line excitation (206). Similarly, ground state depletion followed by individual molecule return (GSDIM), utilizing the transitions between the fluorophores singlet and triplet states as a stochastic on-off switch, achieved multiplexed super-resolution imaging of three and two proteins in fixed and live cells, respectively (203). In another study, combination of direct STORM (dSTORM) with photoactivation localization microscopy (PALM) enabled simultaneous triple-color super-resolution imaging of the two subunits of type I interferon receptors and actin in live HeLa cells (155). While the obtained three-color super-resolution images integrated 1,000 frames taken within 90 seconds, for many nano-scale dynamics a faster temporal resolution is needed, imposing a compromise on the signal-to-noise ratio. Using dual color STED microscopy, the nano-scale dynamics of epidermal growth factor (EGF) and EGF receptor (EGFR) was monitored in live cells at a temporal resolution of about 12 seconds

(156). Similarly, dual color STED imaging of synapses in live cells was reported (207).

High-Throughput Multiplexed Imaging

Multiplexed imaging overcomes inter-cellular and intracellular variability since it monitors the state of a protein network in each optically resolvable area unit, rather than integrating it over the cell (e.g., as in FCM) or over a cell population (e.g., as in Western blot). On the other hand, high-throughput measurements of only one component per object (a cell in a population or areas within a cell) can by itself uncover the heterogeneity of these objects in respect to the level of this component. The combination of these two aspects, multiplexing and high-throughput, allows uncovering the statistical relations between the measured components. High-throughput multiplexed measurements facilitate the identification and characterization of cell subpopulations based on multi-parametric classifications (20,22,208). In the case of a cell population responding to a stimulus, the emergence of discrete subpopulations indicates important properties of the system, such as bistability and multistability—having two or more stable steady states for the same input conditions (209). High-throughput multiplexed imaging can identify sub-populations of cells based on the distinct patterns of protein localization. In addition, multiplexed imaging can uncover molecular diversity between intracellular structures, like adhesion sites or endosomes (51,53,210). If these structures are plentiful within cells, a large sampling can be obtained already with the analysis of few cells. Still, in order to overcome cell-to-cell variability, it is valuable to infer inter-structure diversities based on a large number of cells.

Molecular heterogeneity has in many cases a functional significance from which causality can be derived (211–213). For example, variation analysis within a subpopulation can be used to determine the presence of positive and negative feedbacks (Fig. 4a) (212). However in many cases high-throughput quantification of a single observable is insufficient for untangling the source of the variation. For example, the strength in the response to a given growth factor might be related to the expression level of the different components, in particular to the corresponding receptor. High-throughput multiplexed measurements can capture multi-dimensional statistical relations between the labeled components, thus to uncover the source of variation. Moreover, co-measuring the variances in the levels of multiple components facilitates network construction approaches (214,215). Although predictions based on observational data cannot replace those derive from perturbation analysis, they are valuable for confining the possible models and designing future experiments.

Flow based methods provide unsurpassed throughput and multiplexity per cell. Such combination enabled, for example, to reveal that cancer cells of the same patient have distinct set of alterations in their signaling networks (28). However, as aforementioned, FCM and mass cytometry do not provide subcellular resolution. Since the alterations in the state of a protein network could be manifested by its spatial organization within cells, multiplexed imaging is required to capture these diversities. To add the spatial dimension, in image flow cytometry the point detector is replaced by a high-speed fluorescence camera, thus adding morphometric characterization of cells to the obtained parameters (48,216–219). The intracellular (co)-localization of proteins and organelles can be therefore observed, enabling the quantification of spatially organized processes. However, additionally, FCM, image cytometry, and mass cytometry do not allow measuring in a controlled manner the same cell multiple times. In FCM and image cytometry the same population could be re-analyzed but single cells cannot be tracked across these measurements, thereby making it impossible to follow molecular processes in the same cell. Such time-lapse quantifications are of relevance, for example, for determining the fate of distinct populations upon stimulation and are central for understanding how the network transits from one molecular state to another.

Automated microscopy based approaches can provide temporal information of single cell as any cell can be addressed by its position and revisited periodically (220,221). Also, unlike flow-based techniques, high-throughput microscopy can be applied for studying physiological processes in adhesive cells, like adhesion and migration (222–224). Image registration methods can be used when monitoring a cellular process provided that its typical time scale is slower than the imaging rate. Functional imaging can quantify molecular interactions and modification state of proteins directly inside the cell (212,225). In this way a state map, consisting of population evolution of the different interacting or modified proteins, can be overlaid with a topographic map of proteins. For example Förster resonance energy transfer (FRET) measured by fluorescence lifetime imaging microscopy (FLIM), provides accurate imaging of PTM with subcellular resolution (Fig. 4a) (226). In contrast to phenotypic screenings, this method directly measures the molecular states of the components, thereby overcomes a possible phenotype-level robustness of the system. More importantly, being a quantitative technique it enables to investigate causal relationships between proteins from perturbation experiments.

Other types functional imaging techniques have also been implemented in automated microscopy (227–229). For example, fluorescence anisotropy imaging, which monitors the depolarization in the emission due to homoFRET and thus provides valuable information about the degree of clustering of proteins in the plasma membrane and subcellular compartments (227–231). The total acquisition time in automated high-throughput microscopy is still order of magnitudes longer than in flow-based measurements. However recent advances in tissue scanners, such as those used in histology, allow imaging a complete microscopy slide with 40× transmission microscopy in a few minutes. Similar advances are expected to facilitate further high-throughout functional imaging. FCS and FCCS have also been implemented in high-throughput mode providing previously inaccessible information (232). Some of these concepts and techniques are finding their way in whole-organism developmental studies (233,234). The ability to quantify in an automated manner a large number

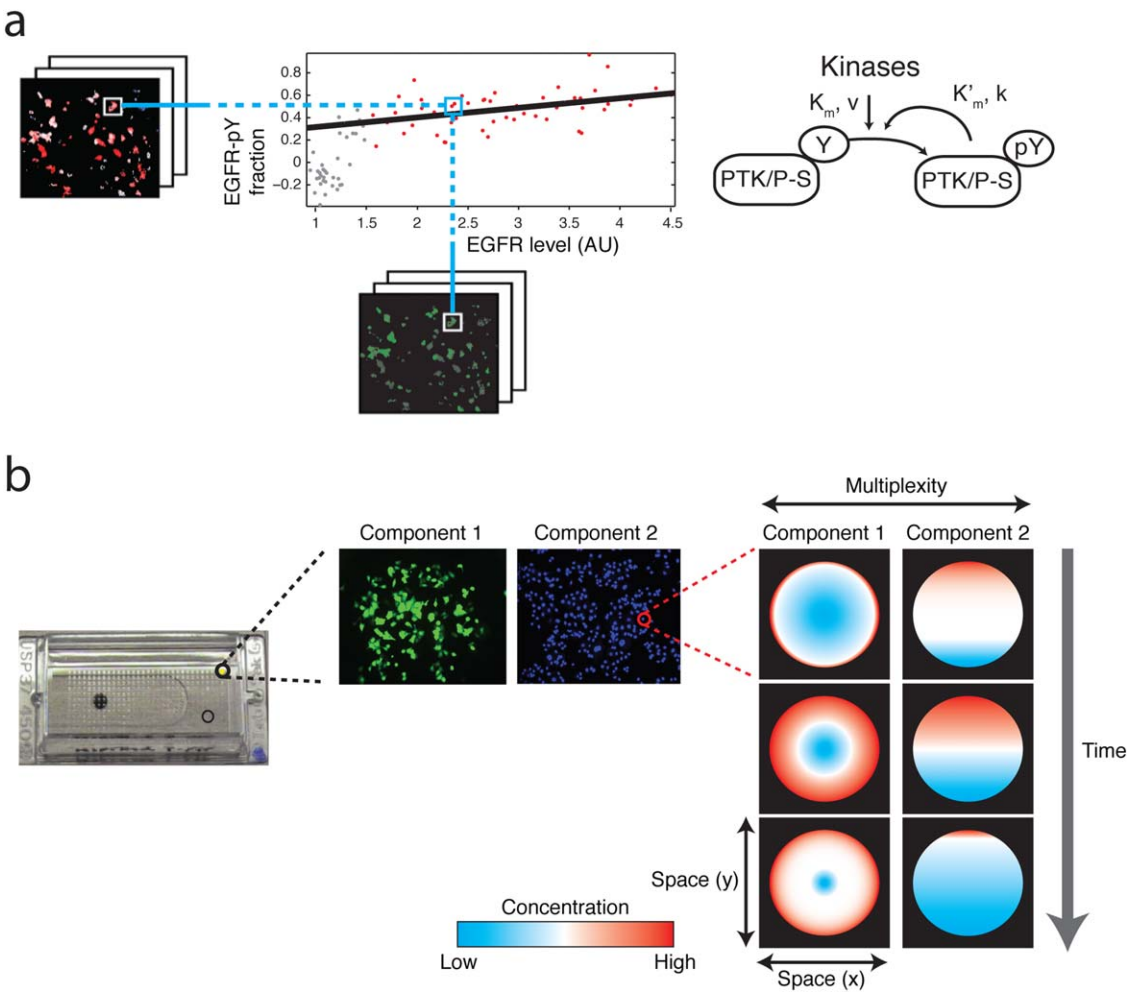

Figure 4. High-throughput microscopy and multiplexed imaging. **(a)** The molar fraction of phosphorylated EGFR (EGFR-pY) was imaged in a large number of single cells by quantifying the FRET between Cy3.5 conjugated to anti-phosphotyrosine antibody and YFP-EGFR. Plotting this fraction versus the intensity of YFP-EGFR in the different imaged cells revealed a positive correlation between the two parameters (212). Such positive correlation indicates that EGFR is embedded in a positive feedback loop (212). Reaction scheme for protein tyrosine kinase and phosphatase substrate (PTK/P-S) with a tyrosine (Y) that can be phosphorylated (pY) by the action of an external kinase with Michaelis constant Km and maximum rate v. Additionally, there is an autocatalytic kinase reaction with constants Km′ and k. (**b**) Illustrative example of multiplexed high-throughput microscopy with high spatial and temporal resolutions. Imaging two components in each cell at a sufficient temporal and spatial resolution could resolve the differential response to stimulus. However, imaging the cell with high spatial resolution reduces the throughput, since a lower number of cells would be captured in each frame. Similarly, high temporal resolution implies a longer period of time spent for each field, therefore also reducing the throughput. Multiplexity reduces the throughput as well, since each component requires a separated image acquisition. Reproduced with modifications from Grecco et al. 2010 (212). [Color figure can be viewed in the online issue which is available at wileyonlinelibrary.com]

of zebrafish or Drosophila embryos facilitates robust variation analysis of these organisms.

Summary And Outlook

Since the discovery and first observations of cells by Hooke and Leeuwenhoek in the 17th century, the endeavor to see a cell is in fact still ongoing, now more intensively than ever. In the systems biology era, the central question became how molecular events within the cell give collectively rise to cellular functionalities. However a fundamental challenge to address this question arises from the large number of different proteins that are involved in cellular processes, their spatiotemporal dynamics and cell-to-cell variability. Multiplexed imaging is the key approach to confront this challenge, yet it faces fundamental difficulties of its own due to trade-offs between multiplexity, spatial resolution, temporal resolution and throughput. The ultimate aspiration to co-image all biochemical species that are relevant for a complex cellular process within intact cells is still far from being achieved. Yet, we can be encouraged by the persistent improvements in multiplexed imaging, attributed to better and more versatile fluorophores, labeling approaches, detectors, high-throughput microscopy instrumentations, data handling and data analysis.

Developing further orthogonal approaches for live cell labeling of tagged proteins with small, bright and photostable fluorophores with narrow emission spectra is a promising

path to improve multiplexed imaging in live cells. The recent CRISPR/Cas9 technology enables endogenous tagging of the target proteins, thereby considerably strengthens this direction (235–238). Further developments of infrared fluorophores for live cell imaging are plausible to take place, thereby further enlarging the usable part of the spectra and increase the number of components that could be co-imaged. On the instrumentation side, the combination of white light lasers with AOBS provides an unprecedented flexibility in setting the optimal imaging channels, thereby facilitating the accessibility and applicability of multiplexity imaging. The continuous advances in the semiconductor industry are providing novel low-noise and highly sensitive detectors with larger dynamic range. High-throughput with high multiplexity and high spatiotemporal resolution (Fig. 4b) is inherently limited, but could be improved by massively parallelized acquisition. Harvesting high-throughput multiplexed image data will require increasingly stronger parallel computations for image analysis, in order to recognize intracellular structures in each component channel, match them across the channels and track them along the time points. Explorations of the obtained multidimensional data would benefit from the progress in machine learning, in particular deep learning, algorithms for learning and capturing complex spatiotemporal patterns of protein networks and their relations with cellular behaviors (239–243). Considering the high-dimensionality and explosion of data size obtainable by brute-force high-throughput multiplexed imaging, an intriguing possibility would be coupling in a feedback the image acquisition with computational deep-learning analysis. Such coupling can enable to automate machine-based explorations of the multiplexed labeled cells, accordingly automating gradual dimensionality reduction in data acquisition and model discovery—already at the level of data acquisition. The current research on this variety of topics and the positive feedback between technological capabilities and biological questions will plausibly push further in the foreseen future the boundaries of multiplexed imaging and thereby of our understanding of cells.

Literature Cited

1. Zamir E, Bastiaens PI. Reverse engineering intracellular biochemical networks. Nat Chem Biol 2008;4:643−647.
2. Kholodenko BN, Kiyatkin A, Bruggeman FJ, Sontag E, Westerhoff HV, Hoek JB. Untangling the wires: A strategy to trace functional interactions in signaling and gene networks. Proc Natl Acad Sci U S A 2002;99:12841−12846.
3. Gangaraju VK, Lin H. MicroRNAs: Key regulators of stem cells. Nat Rev Mol Cell Biol 2009;10:116−125.
4. Rottiers V, Naar AM. MicroRNAs in metabolism and metabolic disorders. Nat Rev Mol Cell Biol 2012;13:239−250.
5. Ambros V. microRNAs: Tiny regulators with great potential. Cell 2001;107:823−826.
6. Nishida M, Maruyama Y, Tanaka R, Kontani K, Nagao T, Kurose H. G alpha(i) and G alpha(o) are target proteins of reactive oxygen species. Nature 2000;408:492−495.
7. Berridge MJ, Bootman MD, Roderick HL. Calcium signalling: Dynamics, homeostasis and remodelling. Nat Rev Mol Cell Biol 2003;4:517−529.
8. Saltel F, Mortier E, Hytonen VP, Jacquier MC, Zimmermann P, Vogel V, Liu W, Wehrle-Haller B. New PI(4,5)P2- and membrane proximal integrin-binding motifs in the talin head control beta3-integrin clustering. J Cell Biol 2009;187:715−731.
9. Jagannathan-Bogdan M, Zon LI. Hematopoiesis. Development 2013;140:2463−2467.
10. Trapnell C. Defining cell types and states with single-cell genomics. Genome Res 2015;25:1491−1498.
11. Rothenberg EV. Stepwise specification of lymphocyte developmental lineages. Curr Opin Genet Dev 2000;10:370−379.
12. Elowitz MB, Levine AJ, Siggia ED, Swain PS. Stochastic gene expression in a single cell. Science 2002;297:1183–1186.
13. Ohnishi Y, Huber W, Tsumura A, Kang M, Xenopoulos P, Kurimoto K, Oles AK, Arauzo-Bravo MJ, Saitou M, Hadjantonakis AK, et al. Cell-to-cell expression variability followed by signal reinforcement progressively segregates early mouse lineages. Nat Cell Biol 2014;16:27–37.
14. Flusberg DA, Sorger PK. Surviving apoptosis: Life-death signaling in single cells. Trends Cell Biol 2015;25:446−458.
15. Wieczorek J, Malik-Sheriff RS, Fermin Y, Grecco HE, Zamir E, Ickstadt K. Uncovering distinct protein-network topologies in heterogeneous cell populations. BMC Syst Biol 2015;9:24
16. Spencer SL, Gaudet S, Albeck JG, Burke JM, Sorger PK. Non-genetic origins of cell-to-cell variability in TRAIL-induced apoptosis. Nature 2009;459:428−432.
17. Paek AL, Liu JC, Loewer A, Forrester WC, Lahav G. Cell-to-cell variation in p53 dynamics leads to fractional killing. Cell 2016;165:631–642.
18. Gaudet S, Miller-Jensen K. Redefining Signaling Pathways with an Expanding Single-Cell Toolbox. Trends Biotechnol 2016, in press. [PMID: 26968612.].
19. Shalek AK, Satija R, Adiconis X, Gertner RS, Gaublomme JT, Raychowdhury R, Schwartz S, Yosef N, Malboeuf C, Lu D, et al. Single-cell transcriptomics reveals bimodality in expression and splicing in immune cells. Nature 2013;498:236−240.
20. Khoo BL, Chaudhuri PK, Ramalingam N, Tan DS, Lim CT, Warkiani ME. Single-cell profiling approaches to probing tumor heterogeneity. Int J Cancer 2016, in press. [PMID: 26789729].
21. Spiller DG, Wood CD, Rand DA, White MR. Measurement of single-cell dynamics. Nature 2010;465:736−745.
22. Bendall SC, Nolan GP. From single cells to deep phenotypes in cancer. Nat Biotechnol 2012;30:639−647.
23. Edwards BS, Oprea T, Prossnitz ER, Sklar LA. Flow cytometry for high-throughput, high-content screening. Curr Opin Chem Biol 2004;8:392−398.
24. Brown M, Wittwer C. Flow cytometry: Principles and clinical applications in hematology. Clin Chem 2000;46:1221−1229.
25. Zamir E, Geiger B, Cohen N, Kam Z, Katz BZ. Resolving and classifying haematopoietic bone-marrow cell populations by multi-dimensional analysis of flow-cytometry data. Br J Haematol 2005;129:420−431.
26. Hale MB, Nolan GP. Phospho-specific flow cytometry: Intersection of immunology and biochemistry at the single-cell level. Curr Opin Mol Ther 2006;8:215−224.
27. Krutzik PO, Crane JM, Clutter MR, Nolan GP. High-content single-cell drug screening with phosphospecific flow cytometry. Nat Chem Biol 2008;4:132−142.
28. Irish JM, Hovland R, Krutzik PO, Perez OD, Bruserud O, Gjertsen BT, Nolan GP. Single cell profiling of potentiated phospho-protein networks in cancer cells. Cell 2004;118:217−228.
29. Irish JM, Kotecha N, Nolan GP. Mapping normal and cancer cell signalling networks: Towards single-cell proteomics. Nat Rev Cancer 2006;6:146−155.
30. Krutzik PO, Irish JM, Nolan GP, Perez OD. Analysis of protein phosphorylation and cellular signaling events by flow cytometry: Techniques and clinical applications. Clin Immunol 2004;110:206−221.
31. Forman MA, Gupta RK. Tandem dyes for flow cytometry: Can we overcome quality concerns? MLO Med Lab Obs 2007;39:24–.
32. Hulspas R, Dombkowski D, Preffer F, Douglas D, Kildew-Shah B, Gilbert J. Flow cytometry and the stability of phycoerythrin-tandem dye conjugates. Cytometry A 2009;75A:966−972.
33. Johansson U, Macey M. Tandem dyes: Stability in cocktails and compensation considerations. Cytometry B Clin Cytom 2014;86B:164−174.
34. Le Roy C, Varin-Blank N, Ajchenbaum-Cymbalista F, Letestu R. Flow cytometry APC-tandem dyes are degraded through a cell-dependent mechanism. Cytometry A 2009;75A:882−890.
35. Batard P, Szollosi J, Luescher I, Cerottini JC, MacDonald R, Romero P. Use of phycoerythrin and allophycocyanin for fluorescence resonance energy transfer analyzed by flow cytometry: Advantages and limitations. Cytometry 2002;48:97–105.
36. O'Donnell EA, Ernst DN, Hingorani R. Multiparameter flow cytometry: Advances in high resolution analysis. Immune Netw 2013;13:43–54.
37. Nolan GP. Flow cytometry in the post fluorescence era. Best Pract Res Clin Haematol 2011;24:505−508.
38. Bendall SC, Nolan GP, Roederer M, Chattopadhyay PK. A deep profiler's guide to cytometry. Trends Immunol 2012;33:323−332.
39. Finck R, Simonds EF, Jager A, Krishnaswamy S, Sachs K, Fantl W, Pe'er D, Nolan GP, Bendall SC. Normalization of mass cytometry data with bead standards. Cytometry A 2013;83A:483−494.
40. Fienberg HG, Nolan GP. Mass cytometry to decipher the mechanism of nongenetic drug resistance in cancer. Curr Top Microbiol Immunol 2014;377:85–94.
41. Zivanovic N, Jacobs A, Bodenmiller B. A practical guide to multiplexed mass cytometry. Curr Top Microbiol Immunol 2014;377:95–109.
42. Nassar AF, Wisnewski AV, Raddassi K. Mass cytometry moving forward in support of clinical research: Advantages and considerations. Bioanalysis 2016;8:255−257.
43. Lai L, Ong R, Li J, Albani S. A CD45-based barcoding approach to multiplex mass-cytometry (CyTOF). Cytometry A 2015;87A:369−374.
44. Atkuri KR, Stevens JC, Neubert H. Mass cytometry: A highly multiplexed single-cell technology for advancing drug development. Drug Metab Dispos 2015;43:227−233.
45. Tanner SD, Baranov VI, Ornatsky OI, Bandura DR, George TC. An introduction to mass cytometry: Fundamentals and applications. Cancer Immunol Immunother 2013;62:955−965.
46. Bendall SC, Simonds EF, Qiu P, Amir el AD, Krutzik PO, Finck R, Bruggner RV, Melamed R, Trejo A, Ornatsky OI. and others. Single-cell mass cytometry of

differential immune and drug responses across a human hematopoietic continuum. Science 2011;332:687−696.
47. Ornatsky O, Bandura D, Baranov V, Nitz M, Winnik MA, Tanner S. Highly multiparametric analysis by mass cytometry. J Immunol Methods 2010;361:1–20.
48. Doan HQ, Chinn GM, Jahan-Tigh RR. Flow cytometry ii: Mass and imaging cytometry. J Invest Dermatol 2015;135:e36.
49. Kinkhabwala A, Bastiaens PI. Spatial aspects of intracellular information processing. Curr Opin Genet Dev 2010;20:31–40.
50. Fuller BG, Lampson MA, Foley EA, Rosasco-Nitcher S, Le KV, Tobelmann P, Brautigan DL, Stukenberg PT, Kapoor TM. Midzone activation of aurora B in anaphase produces an intracellular phosphorylation gradient. Nature 2008;453: 1132−1136.
51. Kam Z, Zamir E, Geiger B. Probing molecular processes in live cells by quantitative multidimensional microscopy. Trends Cell Biol 2001;11:329−334.
52. Zamir E, Geiger B. Molecular complexity and dynamics of cell-matrix adhesions. J Cell Sci 2001;114:3583−3590.
53. Zamir E, Geiger B, Kam Z. Quantitative multicolor compositional imaging resolves molecular domains in cell-matrix adhesions. PLoS One 2008;3:e1901.
54. Zamir E, Katz BZ, Aota S, Yamada KM, Geiger B, Kam Z. Molecular diversity of cell-matrix adhesions. J Cell Sci 1999;112:1655−1669.
55. Zamir E, Katz M, Posen Y, Erez N, Yamada KM, Katz BZ, Lin S, Lin DC, Bershadsky A, Kam Z, et al. Dynamics and segregation of cell-matrix adhesions in cultured fibroblasts. Nat Cell Biol 2000;2:191−196.
56. Zamir E, Vartak N, Bastiaens PIH. Oncogenic signaling from the plasma membrane. In: Yarden Y, Tarcic G, editors. Vesicle Trafficking in Cancer. New York: Springer; 2013. pp 57–74.
57. Kholodenko BN, Hancock JF, Kolch W. Signalling ballet in space and time. Nat Rev Mol Cell Biol 2010;11:414−426.
58. Rompp A, Spengler B. Mass spectrometry imaging with high resolution in mass and space. Histochem Cell Biol 2013;139:759−783.
59. Schober Y, Guenther S, Spengler B, Rompp A. High-resolution matrix-assisted laser desorption/ionization imaging of tryptic peptides from tissue. Rapid Commun Mass Spectrom 2012;26:1141−1146.
60. Aichler M, Walch A. MALDI Imaging mass spectrometry: Current frontiers and perspectives in pathology research and practice. Lab Invest 2015;95:422−431.
61. Schwamborn K, Caprioli RM. Molecular imaging by mass spectrometry–looking beyond classical histology. Nat Rev Cancer 2010;10:639−646.
62. Cornett DS, Reyzer ML, Chaurand P, Caprioli RM. MALDI imaging mass spectrometry: Molecular snapshots of biochemical systems. Nat Methods 2007;4:828−833.
63. Giesen C, Wang HA, Schapiro D, Zivanovic N, Jacobs A, Hattendorf B, Schuffler PJ, Grolimund D, Buhmann JM, Brandt S, et al. Highly multiplexed imaging of tumor tissues with subcellular resolution by mass cytometry. Nat Methods 2014;11: 417−422.
64. Robertson J, Jacquemet G, Byron A, Jones MC, Warwood S, Selley JN, Knight D, Humphries JD, Humphries MJ. Defining the phospho-adhesome through the phosphoproteomic analysis of integrin signalling. Nat Commun 2015;6:6265.
65. Geiger T, Zaidel-Bar R. Opening the floodgates: Proteomics and the integrin adhesome. Curr Opin Cell Biol 2012;24:562−558.
66. Bray J. The Communications Miracle: The Telecommunication Pioneers From MORSE to the Information Superhighway. New York, London: Plenum; 1995. xix, 379 p.
67. Neher R, Neher E. Optimizing imaging parameters for the separation of multiple labels in a fluorescence image. J Microsc 2004;213:46–62.
68. Lim SJ, Zahid MU, Le P, Ma L, Entenberg D, Harney AS, Condeelis J, Smith AM. Brightness-equalized quantum dots. Nat Commun 2015;6:8210.
69. Holmstrom KM, Finkel T. Cellular mechanisms and physiological consequences of redox-dependent signalling. Nat Rev Mol Cell Biol 2014;15:411−421.
70. Finkel T. Signal transduction by reactive oxygen species. J Cell Biol 2011;194:7–15.
71. Magidson V, Khodjakov A. Circumventing photodamage in live-cell microscopy. Methods Cell Biol 2013;114:545−560.
72. Kamata H, Honda S, Maeda S, Chang L, Hirata H, Karin M. Reactive oxygen species promote TNFalpha-induced death and sustained JNK activation by inhibiting MAP kinase phosphatases. Cell 2005;120:649−661.
73. Dickinson ME, Bearman G, Tille S, Lansford R, Fraser SE. Multi-spectral imaging and linear unmixing add a whole new dimension to laser scanning fluorescence microscopy. Biotechniques 2001;31:1272, 1274–1276, 1278.
74. Garini Y, Young IT, McNamara G. Spectral imaging: Principles and applications. Cytometry A 2006;69:735−747.
75. Li Q, He X, Wang Y, Liu H, Xu D, Guo F. Review of spectral imaging technology in biomedical engineering: Achievements and challenges. J Biomed Opt 2013;18: 100901.
76. Tsurui H, Nishimura H, Hattori S, Hirose S, Okumura K, Shirai T. Seven-color fluorescence imaging of tissue samples based on Fourier spectroscopy and singular value decomposition. J Histochem Cytochem 2000;48:653−662.
77. Zimmermann T. Spectral imaging and linear unmixing in light microscopy. Adv Biochem Eng Biotechnol 2005;95:245−265.
78. Zimmermann T, Rietdorf J, Pepperkok R. Spectral imaging and its applications in live cell microscopy. FEBS Lett 2003;546:87–92.
79. Bioucas-Dias JM, Plaza A, Dobigeon N, Parente M, Du Q, Gader P, Chanussot J. Hyperspectral unmixing overview: Geometrical, statistical, and sparse regression-based approaches. IEEE J Select Top Appl Earth Observ Remote Sens 2012;5: 354–379.
80. Keshava N. A survey of spectral unmixing algorithms. Lincolin Lab J 2003;14:55–78.
81. Hoppe AD, Shorte SL, Swanson JA, Heintzmann R. Three-dimensional FRET reconstruction microscopy for analysis of dynamic molecular interactions in live cells. Biophys J 2008;95:400−418.
82. Bayani J, Squire J. Multi-color FISH techniques. Curr Protoc Cell Biol 2004;Chapter 22:Unit 22 5.
83. Geigl JB, Uhrig S, Speicher MR. Multiplex-fluorescence in situ hybridization for chromosome karyotyping. Nat Protoc 2006;1:1172−1184.
84. Imataka G, Arisaka O. Chromosome analysis using spectral karyotyping (SKY). Cell Biochem Biophys 2012;62:13−17.
85. Schrock E, du Manoir S, Veldman T, Schoell B, Wienberg J, Ferguson-Smith MA, Ning Y, Ledbetter DH, Bar-Am I, Soenksen D, et al. Multicolor spectral karyotyping of human chromosomes. Science 1996;273:494−497.
86. Speicher MR, Gwyn Ballard S, Ward DC. Karyotyping human chromosomes by combinatorial multi-fluor FISH. Nat Genet 1996;12:368−375.
87. Anderson R. Multiplex fluorescence in situ hybridization (M-FISH). Methods Mol Biol 2010;659:83–97.
88. Bruchez M, Jr., Moronne M, Gin P, Weiss S, Alivisatos AP. Semiconductor nanocrystals as fluorescent biological labels. Science 1998;281:2013−2016.
89. Chan WC, Nie S. Quantum dot bioconjugates for ultrasensitive nonisotopic detection. Science 1998;281:2016−2018.
90. Service RF. Semiconductor beacons light up cell structures. Science 1998;281: 1930−1931.
91. Hotz CZ. Applications of quantum dots in biology: An overview. Methods Mol Biol 2005;303:1–17.
92. Alivisatos AP, Gu W, Larabell C. Quantum dots as cellular probes. Annu Rev Biomed Eng 2005;7:55–76.
93. Jaiswal JK, Simon SM. Potentials and pitfalls of fluorescent quantum dots for biological imaging. Trends Cell Biol 2004;14:497–504.
94. Resch-Genger U, Grabolle M, Cavaliere-Jaricot S, Nitschke R, Nann T. Quantum dots versus organic dyes as fluorescent labels. Nat Methods 2008;5:763−775.
95. Parak WJ, Pellegrino T, Plank C. Labelling of cells with quantum dots. Nanotechnology 2005;16:R9–R25.
96. Goldman ER, Clapp AR, Anderson GP, Uyeda HT, Mauro JM, Medintz IL, Mattoussi H. Multiplexed toxin analysis using four colors of quantum dot fluororeagents. Anal Chem 2004;76:684−688.
97. Wu X, Liu H, Liu J, Haley KN, Treadway JA, Larson JP, Ge N, Peale F, Bruchez MP. Immunofluorescent labeling of cancer marker Her2 and other cellular targets with semiconductor quantum dots. Nat Biotechnol 2003;21:41−46.
98. Sukhanova A, Devy J, Venteo L, Kaplan H, Artemyev M, Oleinikov V, Klinov D, Pluot M, Cohen JH, Nabiev I. Biocompatible fluorescent nanocrystals for immunolabeling of membrane proteins and cells. Anal Biochem 2004;324:60−67.
99. Xing Y, Chaudry Q, Shen C, Kong KY, Zhau HE, Chung LW, Petros JA, O'Regan RM, Yezhelyev MV, Simons JW. and others. Bioconjugated quantum dots for multiplexed and quantitative immunohistochemistry. Nat Protoc 2007;2:1152−1165.
100. Zrazhevskiy P, True LD, Gao X. Multicolor multicycle molecular profiling with quantum dots for single-cell analysis. Nat Protoc 2013;8:1852−1869.
101. Zrazhevskiy P, Gao X. Quantum dot imaging platform for single-cell molecular profiling. Nat Commun 2013;4:1619.
102. Smith AM, Dave S, Nie S, True L, Gao X. Multicolor quantum dots for molecular diagnostics of cancer. Expert Rev Mol Diagn 2006;6:231−244.
103. Boncompain G, Divoux S, Gareil N, de Forges H, Lescure A, Latreche L, Mercanti V, Jollivet F, Raposo G, Perez F. Synchronization of secretory protein traffic in populations of cells. Nat Methods 2012;9:493−498.
104. Schubert W. Topological proteomics, toponomics, MELK-technology. Adv Biochem Eng Biotechnol 2003;83:189–209.
105. Koczan D, Thiesen HJ. Survey of microarray technologies suitable to elucidate transcriptional networks as exemplified by studying KRAB zinc finger gene families. Proteomics 2006;6:4704−4715.
106. Schubert W. Exploring molecular networks directly in the cell. Cytometry A 2006; 109−112.
107. Schubert W, Bonnekoh B, Pommer AJ, Philipsen L, Bockelmann R, Malykh Y, Gollnick H, Friedenberger M, Bode M, Dress AW. Analyzing proteome topology and function by automated multidimensional fluorescence microscopy. Nat Biotechnol 2006;24:1270−1278.
108. Gerner MY, Kastenmuller W, Ifrim I, Kabat J, Germain RN. Histo-cytometry: A method for highly multiplex quantitative tissue imaging analysis applied to dendritic cell subset microanatomy in lymph nodes. Immunity 2012;37:364−376.
109. Gerner MY, Torabi-Parizi P, Germain RN. Strategically localized dendritic cells promote rapid T cell responses to lymph-borne particulate antigens. Immunity 2015; 42:172−185.
110. Hollman-Hewgley D, Lazare M, Bordwell A, Zebadua E, Tripathi P, Ross AS, Fisher D, Adams A, Bouman D, O'Malley DP, et al. A single slide multiplex assay for the evaluation of classical Hodgkin lymphoma. Am J Surg Pathol 2014;38: 1193−1202.
111. Li C, Ma H, Wang Y, Cao Z, Graves-Deal R, Powell AE, Starchenko A, Ayers GD, Washington MK, Kamath V, et al. Excess PLAC8 promotes an unconventional ERK2-dependent EMT in colon cancer. J Clin Invest 2014;124:2172−2187.
112. Gerdes MJ, Sevinsky CJ, Sood A, Adak S, Bello MO, Bordwell A, Can A, Corwin A, Dinn S, Filkins RJ, et al. Highly multiplexed single-cell analysis of formalin-fixed, paraffin-embedded cancer tissue. Proc Natl Acad Sci U S A 2013;110:11982−11987.
113. Schubert W, Gieseler A, Krusche A, Serocka P, Hillert R. Next-generation biomarkers based on 100-parameter functional super-resolution microscopy TIS. Nat Biotechnol 2012;29:599–610.

114. Bhattacharya S, Mathew G, Ruban E, Epstein DB, Krusche A, Hillert R, Schubert W, Khan M. Toponome imaging system: In situ protein network mapping in normal and cancerous colon from the same patient reveals more than five-thousand cancer specific protein clusters and their subcellular annotation by using a three symbol code. J Proteome Res 2010;9:6112−6125.
115. Schubert W, Gieseler A, Krusche A, Hillert R. Toponome mapping in prostate cancer: Detection of 2000 cell surface protein clusters in a single tissue section and cell type specific annotation by using a three symbol code. J Proteome Res 2009;8:2696−2707.
116. Schubert W. A three-symbol code for organized proteomes based on cyclical imaging of protein locations. Cytometry A 2007;71:352−360. A
117. Schubert W. Advances in toponomics drug discovery: Imaging cycler microscopy correctly predicts a therapy method of amyotrophic lateral sclerosis. Cytometry A 2015;87A:696–703.
118. Pierre S, Scholich K. Toponomics: Studying protein-protein interactions and protein networks in intact tissue. Mol Biosyst 2010;6:641−647.
119. Schubert W, Friedenberger M, Bode M, Krusche A, Hillert R. Functional architecture of the cell nucleus: Towards comprehensive toponome reference maps of apoptosis. Biochim Biophys Acta 2008;1783:2080−2088.
120. Lin JR, Fallahi-Sichani M, Sorger PK. Highly multiplexed imaging of single cells using a high-throughput cyclic immunofluorescence method. Nat Commun 2015; 6:8390
121. Kreis TE, Winterhalter KH, Birchmeier W. In vivo distribution and turnover of fluorescently labeled actin microinjected into human fibroblasts. Proc Natl Acad Sci U S A 1979;76:3814−3818.
122. Kreis TE. Preparation, assay, and microinjection of fluorescently labeled cytoskeletal proteins: Actin, alpha-actinin, and vinculin. Methods Enzymol 1986;134:507−519.
123. Kreis TE, Birchmeier W. Microinjection of fluorescently labeled proteins into living cells with emphasis on cytoskeletal proteins. Int Rev Cytol 1982;75:209−214.
124. Wehland J, Weber K. Distribution of fluorescently labeled actin and tropomyosin after microinjection in living tissue culture cells as observed with TV image intensification. Exp Cell Res 1980;127:397–408.
125. Feramisco JR. Microinjection of fluorescently labeled alpha-actinin into living fibroblasts. Proc Natl Acad Sci U S A 1979;76:3967−3971.
126. Glacy SD. Subcellular distribution of rhodamine-actin microinjected into living fibroblastic cells. J Cell Biol 1983;97:1207−1213.
127. Prasher DC, Eckenrode VK, Ward WW, Prendergast FG, Cormier MJ. Primary structure of the Aequorea victoria green-fluorescent protein. Gene 1992;111:229−233.
128. Chalfie M, Tu Y, Euskirchen G, Ward WW, Prasher DC. Green fluorescent protein as a marker for gene expression. Science 1994;263:802−805.
129. Ormo M, Cubitt AB, Kallio K, Gross LA, Tsien RY, Remington SJ. Crystal structure of the Aequorea victoria green fluorescent protein. Science 1996;273:1392−1395.
130. Yang F, Moss LG, Phillips GN. Jr. The molecular structure of green fluorescent protein. Nat Biotechnol 1996;14:1246−1251.
131. Misteli T, Spector DL. Applications of the green fluorescent protein in cell biology and biotechnology. Nat Biotechnol 1997;15:961−964.
132. Shaner NC, Steinbach PA, Tsien RY. A guide to choosing fluorescent proteins. Nat Methods 2005;2:905−909.
133. Shaner NC, Patterson GH, Davidson MW. Advances in fluorescent protein technology. J Cell Sci 2007;120:4247−4260.
134. Dean KM, Palmer AE. Advances in fluorescence labeling strategies for dynamic cellular imaging. Nat Chem Biol 2014;10:512−523.
135. Muller-Taubenberger A, Anderson KI. Recent advances using green and red fluorescent protein variants. Appl Microbiol Biotechnol 2007;77:1–12.
136. Olenych SG, Claxton NS, Ottenberg GK, Davidson MW. The fluorescent protein color palette. Curr Protoc Cell Biol 2007;Chapter 21:Unit 21 5.
137. Matz MV, Lukyanov KA, Lukyanov SA. Family of the green fluorescent protein: Journey to the end of the rainbow. Bioessays 2002;24:953−959.
138. Chudakov DM, Matz MV, Lukyanov S, Lukyanov KA. Fluorescent proteins and their applications in imaging living cells and tissues. Physiol Rev 2010;90:1103−1163.
139. DeBiasio R, Bright GR, Ernst LA, Waggoner AS, Taylor DL. Five-parameter fluorescence imaging: Wound healing of living Swiss 3T3 cells. J Cell Biol 1987;105: 1613−1622.
140. Grimm JB, English BP, Chen J, Slaughter JP, Zhang Z, Revyakin A, Patel R, Macklin JJ, Normanno D, Singer RH, et al. A general method to improve fluorophores for live-cell and single-molecule microscopy. Nat Methods 2015;12:244−250, 3 p following 250.
141. Hoffmann C, Gaietta G, Zurn A, Adams SR, Terrillon S, Ellisman MH, Tsien RY, Lohse MJ. Fluorescent labeling of tetracysteine-tagged proteins in intact cells. Nat Protoc 2010;5:1666−1677.
142. Crivat G, Taraska JW. Imaging proteins inside cells with fluorescent tags. Trends Biotechnol 2012;30:8–16.
143. Jing C, Cornish VW. Chemical tags for labeling proteins inside living cells. Acc Chem Res 2011;44:784−792.
144. Griffin BA, Adams SR, Tsien RY. Specific covalent labeling of recombinant protein molecules inside live cells. Science 1998;281:269−272.
145. Adams SR, Campbell RE, Gross LA, Martin BR, Walkup GK, Yao Y, Llopis J, Tsien RY. New biarsenical ligands and tetracysteine motifs for protein labeling in vitro and in vivo: Synthesis and biological applications. J Am Chem Soc 2002;124:6063−6076.
146. O'Hare HM, Johnsson K, Gautier A. Chemical probes shed light on protein function. Curr Opin Struct Biol 2007;17:488−494.
147. Zurn A, Klenk C, Zabel U, Reiner S, Lohse MJ, Hoffmann C. Site-specific, orthogonal labeling of proteins in intact cells with two small biarsenical fluorophores. Bioconjug Chem 2010;21:853−859.
148. Gautier A, Juillerat A, Heinis C, Correa IR, Jr., Kindermann M, Beaufils F, Johnsson K. An engineered protein tag for multiprotein labeling in living cells. Chem Biol 2008;15:128−136.
149. Los GV, Encell LP, McDougall MG, Hartzell DD, Karassina N, Zimprich C, Wood MG, Learish R, Ohana RF, Urh M, et al. HaloTag: A novel protein labeling technology for cell imaging and protein analysis. ACS Chem Biol 2008;3:373−382.
150. Lukinavicius G, Reymond L, Johnsson K. Fluorescent labeling of SNAP-tagged proteins in cells. Methods Mol Biol 2015;1266:107−118.
151. Hinner MJ, Johnsson K. How to obtain labeled proteins and what to do with them. Curr Opin Biotechnol 2010;21:766−776.
152. Knight SC, Xie L, Deng W, Guglielmi B, Witkowsky LB, Bosanac L, Zhang ET, El Beheiry M, Masson JB, Dahan M, et al. Dynamics of CRISPR-Cas9 genome interrogation in living cells. Science 2015;350:823−826.
153. Lai YT, Chang YY, Hu L, Yang Y, Chao A, Du ZY, Tanner JA, Chye ML, Qian C, Ng KM, et al. Rapid labeling of intracellular His-tagged proteins in living cells. Proc Natl Acad Sci U S A 2015;112:2948−2953.
154. Stagge F, Mitronova GY, Belov VN, Wurm CA, Jakobs S. SNAP-, CLIP- and Halotag labelling of budding yeast cells. PLoS One 2013;8:e78745
155. Wilmes S, Staufenbiel M, Lisse D, Richter CP, Beutel O, Busch KB, Hess ST, Piehler J. Triple-color super-resolution imaging of live cells: Resolving submicroscopic receptor organization in the plasma membrane. Angew Chem Int Ed Engl 2012;51:4868−4871.
156. Pellett PA, Sun X, Gould TJ, Rothman JE, Xu MQ, Correa IR Jr., Bewersdorf J. Two-color STED microscopy in living cells. Biomed Opt Express 2011;2:2364−2371.
157. Klein T, Loschberger A, Proppert S, Wolter S, van de Linde S, Sauer M. Live-cell dSTORM with SNAP-tag fusion proteins. Nat Methods 2011;8:7–9.
158. Jones SA, Shim SH, He J, Zhuang X. Fast, three-dimensional super-resolution imaging of live cells. Nat Methods 2011;8:499–508.
159. Hayashi-Takanaka Y, Yamagata K, Wakayama T, Stasevich TJ, Kainuma T, Tsurimoto T, Tachibana M, Shinkai Y, Kurumizaka H, Nozaki N, et al. Tracking epigenetic histone modifications in single cells using Fab-based live endogenous modification labeling. Nucleic Acids Res 2011;39:6475−6488.
160. Stasevich TJ, Hayashi-Takanaka Y, Sato Y, Maehara K, Ohkawa Y, Sakata-Sogawa K, Tokunaga M, Nagase T, Nozaki N, McNally JG, et al. Regulation of RNA polymerase II activation by histone acetylation in single living cells. Nature 2014;516:272−275.
161. McNeil PL, Warder E. Glass beads load macromolecules into living cells. J Cell Sci 1987;88:669−678.
162. Kimura H, Hayashi-Takanaka Y, Stasevich TJ, Sato Y. Visualizing posttranslational and epigenetic modifications of endogenous proteins in vivo. Histochem Cell Biol 2015;144:101−109.
163. Tanenbaum ME, Gilbert LA, Qi LS, Weissman JS, Vale RD. A protein-tagging system for signal amplification in gene expression and fluorescence imaging. Cell 2014;159:635−646.
164. Ries J, Schwille P. Fluorescence correlation spectroscopy. Bioessays 2012;34:361−368.
165. Hoffmann JE, Fermin Y, Stricker RL, Ickstadt K, Zamir E. Symmetric exchange of multi-protein building blocks between stationary focal adhesions and the cytosol. Elife 2014;3:e02257.
166. Zamir E, Lommerse PH, Kinkhabwala A, Grecco HE, Bastiaens PI. Fluorescence fluctuations of quantum-dot sensors capture intracellular protein interaction dynamics. Nat Methods 2010;7:295−298.
167. Bacia K, Kim SA, Schwille P. Fluorescence cross-correlation spectroscopy in living cells. Nat Methods 2006;3:83−89.
168. Bacia K, Schwille P. Practical guidelines for dual-color fluorescence cross-correlation spectroscopy. Nat Protoc 2007;2:2842−2856.
169. Hwang LC, Gosch M, Lasser T, Wohland T. Simultaneous multicolor fluorescence cross-correlation spectroscopy to detect higher order molecular interactions using single wavelength laser excitation. Biophys J 2006;91:715−727.
170. Blades ML, Grekova E, Wobma HM, Chen K, Chan WC, Cramb DT. Three-color fluorescence cross-correlation spectroscopy for analyzing complex nanoparticle mixtures. Anal Chem 2012;84:9623−9631.
171. Wobma HM, Blades ML, Grekova E, McGuire DL, Chen K, Chan WC, Cramb DT. The development of direct multicolour fluorescence cross-correlation spectroscopy: Towards a new tool for tracking complex biomolecular events in real-time. Phys Chem Chem Phys 2012;14:32904.
172. Heinze KG, Jahnz M, Schwille P. Triple-color coincidence analysis: One step further in following higher order molecular complex formation. Biophys J 2004;86:506−516.
173. Hur KH, Chen Y, Mueller JD. Characterization of ternary protein systems in vivo with tricolor heterospecies partition analysis. Biophys J 2016;110:1158−1167.
174. Chen Y, Muller JD. Determining the stoichiometry of protein heterocomplexes in living cells with fluorescence fluctuation spectroscopy. Proc Natl Acad Sci U S A 2007;104:3147−3152.
175. Chen Y, Johnson J, Macdonald P, Wu B, Mueller JD. Observing protein interactions and their stoichiometry in living cells by brightness analysis of fluorescence fluctuation experiments. Methods Enzymol 2010;472:345−363.
176. Digman MA, Gratton E. Analysis of diffusion and binding in cells using the RICS approach. Microsc Res Tech 2009;72:323−332.
177. Kolin DL, Wiseman PW. Advances in image correlation spectroscopy: Measuring number densities, aggregation states, and dynamics of fluorescently labeled macromolecules in cells. Cell Biochem Biophys 2007;49:141−164.
178. Krieger JW, Singh AP, Bag N, Garbe CS, Saunders TE, Langowski J, Wohland T. Imaging fluorescence (cross-) correlation spectroscopy in live cells and organisms. Nat Protoc 2015;10:1948−1974.
179. Dorlich RM, Chen Q, Niklas Hedde P, Schuster V, Hippler M, Wesslowski J, Davidson G, Nienhaus GU. Dual-color dual-focus line-scanning FCS for quantitative analysis of receptor-ligand interactions in living specimens. Sci Rep 2015;5:10149.

180. Hendrix J, Lamb DC. Implementation and application of pulsed interleaved excitation for dual-color FCS and RICS. Methods Mol Biol 2014;1076:653−682.
181. Digman MA, Wiseman PW, Choi C, Horwitz AR, Gratton E. Stoichiometry of molecular complexes at adhesions in living cells. Proc Natl Acad Sci U S A 2009; 106:2170−2175.
182. Zaidel-Bar R, Itzkovitz S, Ma'ayan A, Iyengar R, Geiger B. Functional atlas of the integrin adhesome. Nat Cell Biol 2007;9:858−867.
183. Legate KR, Montanez E, Kudlacek O, Fassler R. ILK, PINCH and parvin: The tIPP of integrin signalling. Nat Rev Mol Cell Biol 2006;7:20–31.
184. Chorev DS, Moscovitz O, Geiger B, Sharon M. Regulation of focal adhesion formation by a vinculin-Arp2/3 hybrid complex. Nat Commun 2014;5:3758
185. Koster J, Zamir E, Rahmann S. Efficiently mining protein interaction dependencies from large text corpora. Integr Biol (Camb) 2012;4:805−812.
186. McKay MM, Ritt DA, Morrison DK. Signaling dynamics of the KSR1 scaffold complex. Proc Natl Acad Sci U S A 2009;106:11022−11027.
187. Maeder CI, Hink MA, Kinkhabwala A, Mayr R, Bastiaens PI, Knop M. Spatial regulation of Fus3 MAP kinase activity through a reaction-diffusion mechanism in yeast pheromone signalling. Nat Cell Biol 2007;9:1319−1326.
188. Hell SW, Wichmann J. Breaking the diffraction resolution limit by stimulated emission: Stimulated-emission-depletion fluorescence microscopy. Opt Lett 1994;19:780−782.
189. Betzig E, Patterson GH, Sougrat R, Lindwasser OW, Olenych S, Bonifacino JS, Davidson MW, Lippincott-Schwartz J, Hess HF. Imaging intracellular fluorescent proteins at nanometer resolution. Science 2006;313:1642−1645.
190. Betzig E. Proposed method for molecular optical imaging. Opt Lett 1995;20:237−239.
191. Dickson RM, Cubitt AB, Tsien RY, Moerner WE. On/off blinking and switching behaviour of single molecules of green fluorescent protein. Nature 1997;388:355−358.
192. Galbraith CG, Galbraith JA. Super-resolution microscopy at a glance. J Cell Sci 2011;124:1607−1611.
193. Tam J, Cordier GA, Borbely JS, Sandoval Alvarez A, Lakadamyali M. Cross-talk-free multi-color STORM imaging using a single fluorophore. PLoS One 2014;9:e101772.
194. Valley CC, Liu S, Lidke DS, Lidke KA. Sequential superresolution imaging of multiple targets using a single fluorophore. PLoS One 2015;10:e0123941.
195. Jungmann R, Avendano MS, Woehrstein JB, Dai M, Shih WM, Yin P. Multiplexed 3D cellular super-resolution imaging with DNA-PAINT and Exchange-PAINT. Nat Methods 2014;11:313−318.
196. Bates M, Huang B, Dempsey GT, Zhuang X. Multicolor super-resolution imaging with photo-switchable fluorescent probes. Science 2007;317:1749−1753.
197. Zhang Z, Kenny SJ, Hauser M, Li W, Xu K. Ultrahigh-throughput single-molecule spectroscopy and spectrally resolved super-resolution microscopy. Nat Methods 2015;12:935−938.
198. Han KY, Ha T. Dual-color three-dimensional STED microscopy with a single high-repetition-rate laser. Opt Lett 2015;40:2653−2656.
199. Osseforth C, Moffitt JR, Schermelleh L, Michaelis J. Simultaneous dual-color 3D STED microscopy. Opt Express 2014;22:7028−7039.
200. Buckers J, Wildanger D, Vicidomini G, Kastrup L, Hell SW. Simultaneous multi-lifetime multi-color STED imaging for colocalization analyses. Opt Express 2011; 19:3130−3143.
201. Godin AG, Lounis B, Cognet L. Super-resolution microscopy approaches for live cell imaging. Biophys J 2010;107:1777−1784.
202. Fernandez-Suarez M, Ting AY. Fluorescent probes for super-resolution imaging in living cells. Nat Rev Mol Cell Biol 2008;9:929−943.
203. Testa I, Wurm CA, Medda R, Rothermel E, von Middendorf C, Folling J, Jakobs S, Schonle A, Hell SW, Eggeling C. Multicolor fluorescence nanoscopy in fixed and living cells by exciting conventional fluorophores with a single wavelength. Biophys J 2010;99:2686−2694.
204. Bossi M, Folling J, Belov VN, Boyarskiy VP, Medda R, Egner A, Eggeling C, Schonle A, Hell SW. Multicolor far-field fluorescence nanoscopy through isolated detection of distinct molecular species. Nano Lett 2008;8:2463−2468.
205. Schonle A, Hell SW. Fluorescence nanoscopy goes multicolor. Nat Biotechnol 2007; 25:1234−1235.
206. Shim SH, Xia C, Zhong G, Babcock HP, Vaughan JC, Huang B, Wang X, Xu C, Bi GQ, Zhuang X. Super-resolution fluorescence imaging of organelles in live cells with photoswitchable membrane probes. Proc Natl Acad Sci U S A 2012;109: 13978−13983.
207. Tonnesen J, Nadrigny F, Willig KI, Wedlich-Soldner R, Nagerl UV. Two-color STED microscopy of living synapses using a single laser-beam pair. Biophys J 2011;101: 2545−2552.
208. Levine JH, Simonds EF, Bendall SC, Davis KL, Amir el AD, Tadmor MD, Litvin O, Fienberg HG, Jager A, Zunder ER, et al. Data-driven phenotypic dissection of aml reveals progenitor-like cells that correlate with prognosis. Cell 2015;162:184−197.
209. Ferrell JE Jr., Ha SH. Ultrasensitivity part III: Cascades, bistable switches, and oscillators. Trends Biochem Sci 2014;39:612−618.
210. Perret E, Lakkaraju A, Deborde S, Schreiner R, Rodriguez-Boulan E. Evolving endosomes: How many varieties and why? Curr Opin Cell Biol 2005;17:423−434.
211. Colman-Lerner A, Gordon A, Serra E, Chin T, Resnekov O, Endy D, Pesce CG, Brent R. Regulated cell-to-cell variation in a cell-fate decision system. Nature 2005; 437:699–706.
212. Grecco HE, Roda-Navarro P, Girod A, Hou J, Frahm T, Truxius DC, Pepperkok R, Squire A, Bastiaens PI. In situ analysis of tyrosine phosphorylation networks by FLIM on cell arrays. Nat Methods 2010;7:467−472.
213. Altschuler SJ, Wu LF. Cellular heterogeneity: Do differences make a difference? Cell 2010;141:559–563.
214. Munsky B, Neuert G, van Oudenaarden A. Using gene expression noise to understand gene regulation. Science 2012;336:183−187.
215. Sachs K, Perez O, Pe'er D, Lauffenburger DA, Nolan GP. causal protein-signaling networks derived from multiparameter single-cell data. Science 2005;308:523–529.
216. Elliott GS. Moving pictures: Imaging flow cytometry for drug development. Comb Chem High Throughput Screen 2009;12:849−859.
217. Barteneva NS, Fasler-Kan E, Vorobjev IA. Imaging flow cytometry: Coping with heterogeneity in biological systems. J Histochem Cytochem 2012;60:723−733.
218. Samsel L, McCoy JP. Jr. Imaging flow cytometry for the study of erythroid cell biology and pathology. J Immunol Methods 2015;423:52−59.
219. van der Aar AM, Picavet DI, Muller FJ, de Boer L, van Capel TM, Zaat SA, Bos JD, Janssen H, George TC, Kapsenberg ML, et al. Langerhans cells favor skin flora tolerance through limited presentation of bacterial antigens and induction of regulatory T cells. J Invest Dermatol 2013;133:1240−1249.
220. Neumann B, Walter T, Heriche J-K, Bulkescher J, Erfle H, Conrad C, Rogers P, Poser I, Held M, Liebel U, et al. Phenotypic profiling of the human genome by time-lapse microscopy reveals cell division genes. Nature 2010;464:721–727.
221. Simpson JC, Joggerst B, Laketa V, Verissimo F, Cetin C, Erfle H, Bexiga MG, Singan VR, Heriche J-K, Neumann B, et al. Genome-wide RNAi screening identifies human proteins with a regulatory function in the early secretory pathway. Nat Cell Biol 2012;764–774.
222. Naffar-Abu-Amara S, Shay T, Galun M, Cohen N, Isakoff SJ, Kam Z, Geiger B. Identification of novel pro-migratory, cancer-associated genes using quantitative, microscopy-based screening. PLoS One 2008;3:e1457.
223. Winograd-Katz SE, Itzkovitz S, Kam Z, Geiger B. Multiparametric analysis of focal adhesion formation by RNAi-mediated gene knockdown. J Cell Biol 2009;186: 423−436.
224. Paran Y, Ilan M, Kashman Y, Goldstein S, Liron Y, Geiger B, Kam Z. High-throughput screening of cellular features using high-resolution light-microscopy;application for profiling drug effects on cell adhesion. J Struct Biol 2007;158:233−243.
225. Esposito A, Dohm CP, Bahr M, Wouters FS. Unsupervised fluorescence lifetime imaging microscopy for high content and high throughput screening. Mol Cell Proteom 2007;6:1446−1454.
226. Grecco HE, Roda-Navarro P, Verveer PJ. Global analysis of time correlated single photon counting FRET-FLIM data. Opt Express 2009;17:6493–6508.
227. Squire A, Verveer PJ, Rocks O, Bastiaens PI. Red-edge anisotropy microscopy enables dynamic imaging of homo-FRET between green fluorescent proteins in cells. J Struct Biol 2004;147:62−69.
228. Warren SC, Margineanu A, Katan M, Dunsby C, French PM. Homo-FRET based biosensors and their application to multiplexed imaging of signalling events in live cells. Int J Mol Sci 2015;16:14695−14716.
229. Ghosh S, Saha S, Goswami D, Bilgrami S, Mayor S. Dynamic imaging of homo-FRET in live cells by fluorescence anisotropy microscopy. Methods Enzymol 2012; 505:291–327.
230. Bader AN, Hofman EG, Voortman J, en Henegouwen PM, Gerritsen HC. Homo-FRET imaging enables quantification of protein cluster sizes with subcellular resolution. Biophys J 2009;97:2613−2622.
231. de Heus C, Kagie N, Heukers R, van Bergen en Henegouwen PM, Gerritsen HC. Analysis of EGF receptor oligomerization by homo-FRET. Methods Cell Biol 2013; 117:305−321.
232. Wachsmuth M, Conrad C, Bulkescher J, Koch B, Mahen R, Isokane M, Pepperkok R, Ellenberg J. High-throughput fluorescence correlation spectroscopy enables analysis of proteome dynamics in living cells. Nat Biotech 2015;384–389.
233. Gualda EJ, Pereira H, Vale T, Estrada MFo, Brito C Moreno N. SPIM-fluid: Open source light-sheet based platform for high-throughput imaging. Biomedical Optics Express 2015;4447–4456.
234. Savall J, Ho ETW, Huang C, Maxey JR, Schnitzer MJ. Dexterous robotic manipulation of alert adult Drosophila for high-content experimentation. Nat Meth 2015; 657–660.
235. Hsu PD, Lander ES, Zhang F. Development and applications of CRISPR-Cas9 for genome engineering. Cell 2014;157:1262−1278.
236. Mali P, Esvelt KM, Church GM. Cas9 as a versatile tool for engineering biology. Nat Methods 2013;10:957−963.
237. Vandemoortele G, Gevaert K, Eyckerman S. Proteomics in the genome engineering era. Proteomics 2016;16:177−187.
238. Doudna JA, Charpentier E. Genome editing. The new frontier of genome engineering with CRISPR-Cas9. Science 2014;346:1258096.
239. Mamoshina P, Vieira A, Putin E, Zhavoronkov A. Applications of deep learning in biomedicine. Mol Pharm 2016;13:1445−1454.
240. Chen CL, Mahjoubfar A, Tai LC, Blaby IK, Huang A, Niazi KR, Jalali B. Deep Learning in Label-free Cell Classification. Sci Rep 2016;6:21471.
241. Silver D, Huang A, Maddison CJ, Guez A, Sifre L, van den Driessche G, Schrittwieser J, Antonoglou I, Panneershelvam V, Lanctot M, et al. Mastering the game of Go with deep neural networks and tree search. Nature 2016;529:484−489.
242. Kraus OZ, Frey BJ. Computer vision for high content screening. Crit Rev Biochem Mol Biol 2016;51:102−109.
243. Ghahramani Z. Probabilistic machine learning and artificial intelligence. Nature 2015;521:452−459.